

AD-A058 828

PENNSYLVANIA STATE UNIV UNIVERSITY PARK APPLIED RESE--ETC F/G 7/2
FIRST PRINCIPLES PSEUDOPOTENTIAL CALCULATIONS OF ELECTRONIC AND--ETC(U)
JUL 78 R S DAY

N00017-73-C-1418

UNCLASSIFIED

ARL-PSU-TM-78-194

NL

1 of 2

AD
A058 828



AD A0 58828

DDC FILE COPY,

LEVEL II

12

6

FIRST PRINCIPLES PSEUDOPOTENTIAL CALCULATIONS
OF ELECTRONIC AND ATOMIC PROPERTIES OF SOLID
AND LIQUID ALKALI METALS.

10

Richard S. Day

9

Doctoral thesis,

14

ARL-PSU-TM-78-194

Technical Memorandum

File No. 78-194

Jul 1978

Contract No. N00017-73-C-1418

11

Copy No.

6

12 1197.

DDC
RECEIVED
SEP 19 1978
OFFICE

The Pennsylvania State University
Institute for Science and Engineering
APPLIED RESEARCH LABORATORY
Post Office Box 30
State College, PA 16801

Approved for public release
Distribution Unlimited

NAVY DEPARTMENT

NAVAL SEA SYSTEMS COMMAND

391 007

08 09 11 020

mit

UNCLASSIFIED

SECURITY CLASSIFICATION OF THIS PAGE (When Data Entered)

REPORT DOCUMENTATION PAGE		READ INSTRUCTIONS BEFORE COMPLETING FORM
1. REPORT NUMBER TM 78-194✓	2. GOVT ACCESSION NO.	3. RECIPIENT'S CATALOG NUMBER
4. TITLE (and Subtitle) FIRST PRINCIPLES PSEUDOPOTENTIAL CALCULATIONS OF ELECTRONIC AND ATOMIC PROPERTIES OF SOLID AND LIQUID ALKALI METALS		5. TYPE OF REPORT & PERIOD COVERED Ph.D. thesis, November 1978
		6. PERFORMING ORG. REPORT NUMBER TM 78-194
7. AUTHOR(s) Richard S. Day		8. CONTRACT OR GRANT NUMBER(s) N00017-73-C-1418✓
9. PERFORMING ORGANIZATION NAME AND ADDRESS The Pennsylvania State University Applied Research Laboratory✓ P. O. Box 30, State College, PA 16801		10. PROGRAM ELEMENT, PROJECT, TASK AREA & WORK UNIT NUMBERS
11. CONTROLLING OFFICE NAME AND ADDRESS Naval Sea Systems Command Department of the Navy Washington, D. C. 20362		12. REPORT DATE July 10, 1978
		13. NUMBER OF PAGES 125 pages & figures
14. MONITORING AGENCY NAME & ADDRESS (if different from Controlling Office)		15. SECURITY CLASS. (of this report) Unclassified, Unlimited
		15a. DECLASSIFICATION/DOWNGRADING SCHEDULE
16. DISTRIBUTION STATEMENT (of this Report) Approved for public release, distribution unlimited, per NSSC (Naval Sea Systems Command), 8/8/78		
17. DISTRIBUTION STATEMENT (of the abstract entered in Block 20, if different from Report)		
18. SUPPLEMENTARY NOTES		
19. KEY WORDS (Continue on reverse side if necessary and identify by block number)		
20. ABSTRACT (Continue on reverse side if necessary and identify by block number) First principles fully nonlocal pseudopotentials are constructed for the alkali metals Li, Na, and K. The orthogonalization hole contribution to the pseudopotential is treated exactly and comparison with approximate treatments show significant differences. The pseudopotentials are used to calculate various solid and liquid properties of these alkalis. The phonon spectra and elastic shear constants are calculated for the solid metal and are in good agreement with experiment. They are generally within 20% of experiment and		

UNCLASSIFIED

SECURITY CLASSIFICATION OF THIS PAGE(When Data Entered)

20. ABSTRACT (Continued)

in some cases much better agreement is obtained. The liquid structure factor curve, $S(q)$, is calculated using a Monte Carlo technique and the agreement with experiment is excellent. Electrical resistivities of the liquid alkali metals are also calculated using the pseudo-potential and computed liquid structure. The electronic transport properties are calculated for the first time, using the same ion potential to determine the theoretical liquid structure and to describe the electron scattering potential in the solid. The results are in reasonable agreement with experiment considering the first principles nature of the calculation.

Finally, a pseudo-atom model is suggested as a more appropriate means of describing the core-electron states used in constructing the pseudopotential.

ACCESSION for	
NTIS	White Section <input checked="" type="checkbox"/>
PDC	Buff Section <input type="checkbox"/>
UNANNOUNCED	
JUSTIFICATION	
BY	
DISTRIBUTION/AVAILABILITY CODES	
Dist	all and/or SPECIAL
A	-

UNCLASSIFIED

SECURITY CLASSIFICATION OF THIS PAGE(When Data Entered)

The Pennsylvania State University

The Graduate School

Department of Physics

First Principles Pseudopotential Calculations of Electronic
and Atomic Properties of Solid and Liquid Alkali Metals

A Thesis in

Physics

by

Richard S. Day

Submitted in Partial Fulfillment
of the Requirements
for the Degree of

Doctor of Philosophy

November 1978

The signatories below indicate that they have read and approved the thesis of Richard S. Day.

Date of Signature:

10 JULY 1978

26 July 1978

11 July 1978

11 July 1978

11 July 1978

11 July 1978

Signatories:

Paul H. Cutler
Paul H. Cutler, Professor of Physics
Chairman of Committee

R. H. Good, Jr.
R. H. Good, Jr., Head of the
Department of Physics

G. A. Barsch
G. A. Barsch, Professor of Physics
Member of Doctoral Committee

Robert W. Reed
Robert W. Reed, Assistant Professor
of Physics, Member of Doctoral
Committee

Peter B. Shaw
Peter B. Shaw, Associate Professor of
Physics, Member of Doctoral Committee

M. T. Pigott
M. T. Pigott, Professor of Engineering
Research, Member of Doctoral Committee

ABSTRACT

First principles fully nonlocal pseudopotentials are constructed for the alkali metals Li, Na, and K. The orthogonalization hole contribution to the pseudopotential is treated exactly and comparison with approximate treatments show significant differences. The pseudopotentials are used to calculate various solid and liquid properties of these alkalis. The phonon spectra and elastic shear constants are calculated for the solid metal and are in good agreement with experiment. They are generally within 20% of experiment and in some cases much better agreement is obtained. The liquid structure factor curve, $S(q)$, is calculated using a Monte Carlo technique and the agreement with experiment is excellent. Electrical resistivities of the liquid alkali metals are also calculated using the pseudopotential and computed liquid structure. The electronic transport properties are calculated for the first time, using the same ion potential to determine the theoretical liquid structure and to describe the electron scattering potential in the solid. The results are in reasonable agreement with experiment considering the first principles nature of the calculation.

Finally, a pseudo-atom model is suggested as a more appropriate means of describing the core-electron states used in constructing the pseudopotential.

TABLE OF CONTENTS

	Page
ABSTRACT	iii
LIST OF TABLES	vi
LIST OF FIGURES	vii
ACKNOWLEDGMENTS	ix
I. INTRODUCTION AND STATEMENT OF OBJECTIVES	1
II. HISTORICAL NOTE	4
III. THE LINEAR OPTIMIZED PSEUDOPOTENTIAL	8
Pseudopotential Matrix Elements	8
Factorization of the Pseudopotential	12
IV. THE CRYSTALLINE POTENTIAL AND THE PSEUDOPOTENTIAL	14
The Core-Electron Eigenstates	14
The Crystalline Potential	15
V. APPLICATION OF THE PSEUDOPOTENTIAL TO THE CALCULATION OF PROPERTIES OF THE SOLID ALKALIS	17
Phonon Spectra and the Conduction-Core Exchange Interaction	18
Phonon Spectra and the Core-Electron Eigenstates	23
The Conduction-Electron Potential and the Phonon Spectra	27
VI. PHONON SPECTRA AND ELASTIC SHEAR CONSTANTS OF THE SOLID ALKALI METALS	32
Results for Li, Na, and K	32
VII. CALCULATION OF THE LIQUID METAL PROPERTIES OF THE ALKALIS	38
Liquid Metal Structure	38
Methods for Calculating the Liquid Structure	42
The Monte Carlo Calculation and the Markov Chain	43
VIII. THE PAIR POTENTIAL	49
IX. MONTE CARLO RESULTS FOR THE LIQUID STRUCTURE	52
X. LIQUID METAL ELECTRICAL RESISTIVITY	62
XI. POSSIBLE IMPROVEMENTS	64
XII. SUMMARY AND CONCLUSIONS	69

78 09 11 020

TABLE OF CONTENTS (cont.)

	Page
APPENDIX A	
THEORY OF PHONONS FOR BCC STRUCTURE	71
APPENDIX B	
ELASTIC CONSTANTS FOR BODY CENTERED CUBIC MATERIALS	79
APPENDIX C	
THE ORTHOGONALIZATION HOLE	88
APPENDIX D	
SCREENING OF THE PSEUDOPOTENTIAL	95
APPENDIX E	
DERIVATION OF THE LIQUID METAL RESISTIVITY EXPRESSION . . .	100
BIBLIOGRAPHY	104

LIST OF TABLES

Table	Page
1. Experimental versus theoretical eigenvalues for the Li^+ ion and the Na and K atoms	27
2. Elastic shear constants for the simple alkalis Li, Na, and K	37
3. Temperature and density of Li, Na, and K at their melting points	56
4. $S(q)$ values for Li, Na, and K at low q as predicted by Monte Carlo computations	61
5. Theoretical and experimental values for the electrical resistivity for Li, Na, and K at their melting points . .	63
6. Exact versus approximate V^{opw} for Li, Na, and K	93

LIST OF FIGURES

Figure	Page
1. Li phonon spectra showing sensitivity to the conduction-core exchange approximation	20
2. Sensitivity of the phonon spectra of K to the exchange approximation used in the construction of the core electron states	24
3. Demonstration of phonon spectra sensitivity to the core electron eigenvalue E_{nl}	26
4. Exact versus approximate treatment of the orthogonalization hole and its influence upon the Li phonon spectra .	29
5. Phonon spectra for Na calculated with the Hartree and SSTL dielectric screening functions	31
6. Phonon spectra for Li using a Kohn-Sham treatment of the conduction-core exchange and a Hartree dielectric screening function	34
7. Phonon spectra for Na using Lindgren's approximation to the conduction-core exchange and Singwi et al's (1970) dielectric function	35
8. Phonon spectra for K from a pseudopotential using Lindgren's approximation to the conduction-core exchange and Singwi et al's (1970) dielectric screening function .	36
9. Structure factor, $S(q)$, curves for ideal systems	40
10. Model of a two-dimensional liquid with $N = 5$ particles per cell and periodic boundary conditions	40
11. Pair potential curves	50
12. Radial distribution function for Li	53
13. Monte Carlo result for the radial distribution function of Na at its melting point	54
14. Monte Carlo result for the radial distribution function of K at its melting point	55
15. $S(q)$ curve for Li at its melting point	57

LIST OF FIGURES (cont.)

Figure	Page
16. $S(q)$ curve for Na at its melting point	58
17. $S(q)$ curve for K at its melting point	59
18. Volume conserving elastic shears for a bcc system	82
19. Exact $n^{OH}(\vec{r})$ for Li, Na, and K	94

ACKNOWLEDGMENTS

Special thanks are due to the author's adviser, Professor Paul H. Cutler, who suggested this problem and provided advice and encouragement during the course of this research.

The author would also like to thank Mr. Franklin Sun and Dr. Walter F. King, III for helpful discussions relating to this work.

The financial support of the Applied Research Laboratory of The Pennsylvania State University, under contract with the Naval Sea Systems Command, is gratefully acknowledged and in particular the support and encouragement of Professor M. T. Pigott is appreciated.

I. INTRODUCTION AND STATEMENT OF OBJECTIVES

In this thesis, pseudopotential calculations are done for the simple (i.e., no d-electrons) alkali metals Li, Na, and K. These metals were chosen because they are free-electron-like in their behavior and have a small well defined core. They are, therefore, well suited for investigation by the pseudopotential method. Solid and liquid metal properties are calculated for each of the aforementioned alkali metals. The solid properties calculated are the phonon spectra, the pair potentials, and the elastic shear constants. The liquid metal properties calculated include the effective ion-ion potential, the radial distribution function, the static structure factor, and the electrical resistivity of the metal. Both the solid and liquid metal results are in good agreement with experimental evidence.

The pseudopotentials used in these calculations are distinctive in a number of ways. First, all calculations are fully nonlocal throughout all stages of the computation. The only exception is the calculation of the electrical resistivity for the liquid metal which uses the Ziman (1961) local theory discussed in Appendix E. The nonlocality of the pseudopotential means that its matrix element $\langle \vec{k} + \vec{q} | W | \vec{k} \rangle$ depends on the magnitude of \vec{k} as well as the angle between \vec{k} and $\vec{k} + \vec{q}$, and is not restricted to the so-called Fermi sphere approximation (i.e., $|\vec{k}| = k_f$). Use of the nonlocal form of the pseudopotential makes the computer calculations considerably more difficult, but computed results can be quite different if the nonlocality of the pseudopotential is ignored. Secondly, it should be stressed that our pseudopotentials

are first principles which are distinctly different than model or parameterized potentials. The following criteria are implied by the use of the words 'first principles.' A pseudopotential is first principles if the localized core-electron states are explicitly represented by wave functions that are solutions of a Schrödinger equation. These core states are used to construct the ionic charge density and, subsequently, this charge density determines the Coulombic potential of the ion in the crystal. In addition, the crystalline potential is represented by an expression that does not make use of arbitrarily adjustable parameters. The only experimental information used in our calculations, other than fundamental physical constants, is the lattice structure, lattice constant, and the atomic number of the atoms composing the metal.

The basic objective of this thesis is to study the electron-electron and electron-ion interactions which are responsible for determining the physical properties of the alkali metals Li, Na, and K. This is done by determining the sensitivity of the lattice dynamical properties to each of the various contributions to the crystalline potential. As a result of these studies certain contributions to the pseudopotential are treated more rigorously than in previous calculations. Specifically, the charge density and Coulomb potential of the orthogonalization hole (OH), as well as its interaction with the core-electron density are treated exactly for the first time for Li, Na, and K. The results using an 'exact' OH density show that approximate treatments of this particular contribution to the conduction-electron potential are inadequate and that an exact treatment of the OH produces significant

changes in the calculated phonon spectra. Physically, the OH density, $n^{\text{OH}}(r)$, is a part of the conduction-electron charge density which is obtained from the absolute square of the conduction-electron wave function. Also, a thorough analysis is made of the conduction-core exchange interaction and it is found that the Lindgren (1971) exchange potential yields better results in most cases, than the Kohn-Sham (1965) or Slater (1951) potentials. Finally, the electronic transport properties of the liquid alkali metals are calculated for the first time using the same ion potential to determine the theoretical liquid structure and to describe the electron scattering potential in the liquid.

II. HISTORICAL NOTE

Of central importance to pseudopotential theory are the Orthogonalized Plane Waves (OPW) first introduced by Herring (1940). These OPW's are used to represent the conduction-electron states in a crystal. The OPW representation for the conduction eigenstates has the advantage that it converges much faster than a simple plane wave representation. Also, it was noted by Phillips and Kleinman (1959) that the orthogonalization of the plane waves to the core-electron states effectively adds a repulsive term to the crystalline potential. The attractive crystalline potential plus the repulsive orthogonalization term have been collectively labelled as the 'pseudopotential.' This potential is weaker than the crystalline potential which suggests that one can use perturbation theory to solve for the conduction-electron eigenstates. Harrison (1963,1963, 1964) was the first to apply the OPW pseudopotential theory to the calculation of metallic properties. His calculations are noteworthy because he developed his pseudopotentials from first principles. This means that the potential is developed from the wave functions and eigenvalues used to represent the localized core-electron states. Any pseudopotential in which the crystalline potential depends explicitly upon the core-electron states will hereafter be referred to as a Harrison's First Principles (HFP) pseudopotential.

It is instructive to compare the HFP pseudopotential with the 'model' pseudopotential method, which does not construct the potential of an ion in the crystal from the explicit core-electron eigenstates.

Rather, as the name implies, a model potential is constructed to represent the ionic cores in the metal. In both the HFP and model pseudopotentials, the metal is visualized as an array of ions immersed in a compensating conduction-electron sea. Heine and Abrenkov (1965), Animalu (1965), and Ashcroft (1966) were responsible for much of the early development of model pseudopotentials. Heine and Weire (1970) have written an excellent review article on the model pseudopotential method, so we will only briefly touch on the relevant points of this approach. In such calculations, the potential of an ion is represented by a model (i.e., an analytic expression such as a square well potential) with several adjustable parameters that are used to fit the model to known experimental facts. It is hoped that once the parameters have been adjusted to one measurement, then the pseudopotential can be used to predict other atomic and electronic properties of the metal under study.

There are certain model potentials that are quite sophisticated in the way that the parameters are chosen. In particular, Dagens, Rasolt, and Taylor (1975) have developed a clever approach based on the charge density induced by an isolated ion in an electron gas. They adjusted the model potential parameters so that the induced charge density calculated from first order perturbation theory was identical with an exact nonlinear calculation (Dagens, 1972). This is certainly a more fundamental approach than adjusting the model potential to the phonon spectra, elastic constants, or other gross experimental features. However, irrespective of the ingenuity used to adjust the model parameters, one is still working with a model potential and consequently can

not directly obtain fundamental information about the interactions in the crystal. The HFP potential by contrast constructs the crystal potential from wave functions that are solutions of the Schrödinger equation, and thus provides a better means of studying the crystal potential and the interactions that contribute to the crystal potential than does the model pseudopotential method.

Though the HFP pseudopotential method can, in principle, be used to make systematic studies of the interactions existing within a crystal, there have been relatively few such studies done because of the cost and complexity of the calculations. The difficulty of the HFP calculations has limited the practical applications of this technique so that the great majority of pseudopotential calculations use the model potential approach. Since the basic objective of this research is to try to understand some fundamental interactions in the solid and liquid states of metals, the HFP approach has been chosen to systematically study the atomic and electronic properties of the alkali metals Li, Na, and K. The heavier alkalis are not included in this study because the presence of d-electrons in Rb and Cs may require the use of the more complicated Generalized HFP (GHFP) theory which includes the s-d 'hybridization' in the pseudopotential (Harrison, 1969; Moriarity, 1970). The alkalis are ideally suited for study by the pseudopotential method because of their nearly free electron-like behavior and the fact that there is virtually no nearest-neighbor core overlap in the crystal. King and Cutler (1973) have done studies for Li that demonstrated the importance of the conduction-core electron exchange interaction in phonon spectra calculations. More recently, Hafner (1974), and Hafner and

Schmuck (1974) have done studies which also conclude that the conduction-core exchange interaction is an important component of the crystal potential. Hafner's work, however, tended to use parameterized forms of the exchange potential. By contrast, the present work represents a systematic study of the exchange potential in Li, Na, and K using unparameterized versions of approximations to the conduction-core exchange interaction. In addition, for the first time, certain conduction-electron contributions to the crystal potential are treated without approximations; this exact treatment of the conduction-electron potential has not been done before for the alkalis. Specifically, the Orthogonalization Hole density $n^{\text{OH}}(\vec{r})$ is treated exactly and is found to produce significantly different results from previous approximate treatments of $n^{\text{OH}}(\vec{r})$.

III. THE LINEAR OPTIMIZED PSEUDOPOTENTIAL

Pseudopotential Matrix Elements

In this section, a derivation is given of the pseudopotential matrix elements that are used in HFP calculations of the conduction-electron eigenvalues and wave functions. The pseudopotential, denoted by $W(\vec{r})$, will be expressed in terms of the crystal potential $V^C(\vec{r})$, the core-electron eigenstates $\psi_{n\ell}(\vec{r})$, and their corresponding eigenvalues $E_{n\ell}$, where n and ℓ are the principle and angular quantum numbers respectively. The specific forms of $V^C(\vec{r})$, $\psi_{n\ell}(\vec{r})$ and $E_{n\ell}$ will be discussed in later chapters.

In HFP pseudopotential theory, the conduction-electron states are described by linear combinations of OPW's, where a single OPW of wave number $\vec{k} + \vec{q}$ can be written as (assuming no core electron overlaps)

$$|\text{OPW}\rangle = (1 - P) |\vec{k} + \vec{q}\rangle, \quad (1)$$

and $P = \sum_{n\ell} |n\ell\rangle\langle n\ell|$ is a projection operator, which when operating on the plane wave state $|\vec{k} + \vec{q}\rangle$, extracts the components of the plane wave that are not orthogonal to the core-electron states $|n\ell\rangle$. Hence, the OPW in Equation (1) represents a plane wave that has been made orthogonal to the core-electron states. The general expression for a conduction-electron state of wave vector \vec{k} is a linear sum of the OPW's shown in Equation (1)

$$\psi_{\vec{k}}^C(\vec{r}) = \sum_{\vec{q}} a_{\vec{q}}(\vec{k}) (1 - P) |\vec{k} + \vec{q}\rangle. \quad (2)$$

The expansion coefficients $a_{\vec{q}}(\vec{k})$ in Equation (2) are obtained from perturbation theory.

The coefficients are determined by the requirement that $\psi_{\vec{k}}^C(\vec{r})$ is an eigenstate of the crystal Hamiltonian $H = T + V^C$.

$$H\psi_{\vec{k}}^C(\vec{r}) = E_{\vec{k}}\psi_{\vec{k}}^C(\vec{r}) \quad (3)$$

Combining Equations (2) and (3), and with a certain amount of algebra (Harrison, 1966) one can show that Equation (3) may be reexpressed as

$$(T + W(\vec{r}))\phi_{\vec{k}}(\vec{r}) = E_{\vec{k}}\phi_{\vec{k}}(\vec{r}) \quad , \quad (4)$$

where $W(\vec{r})$ is the pseudopotential,

$$W(\vec{r}) = V^C(\vec{r}) + \sum_{n, \ell} (E_{\vec{k}} - E_{n\ell}) |n\ell\rangle\langle n\ell| \quad , \quad (5)$$

and the pseudo-wave function

$$\phi_{\vec{k}}(\vec{r}) = \sum_{\vec{q}} a_{\vec{q}}(\vec{k}) |\vec{k} + \vec{q}\rangle \quad (6)$$

is simply a sum of plane waves. The expansion coefficients $a_{\vec{q}}(\vec{k})$ are the same as previously used in the expression for the conduction eigenstate [i.e., Equation (2)]. $E_{n\ell}$ is the eigenvalue of the n, ℓ core electron state in the crystal environment. Although in principle $\psi_{\vec{k}}^C(\vec{r})$ and $|n\ell\rangle$ should be eigenstates of the same crystal Hamiltonian H , in practice $|n\ell\rangle$ is well approximated by an eigenstate of the free ion. It was Phillips and Kleinman (1959) who first noted the pseudopotential $W(\vec{r})$ is, in general, weaker than the true crystalline potential $V^C(\vec{r})$. This suggests the use of perturbation theory to solve for the eigenstates $\phi_{\vec{k}}(\vec{r})$ and the eigenvalues $E_{\vec{k}}$ of the pseudopotential equation (4). Note that the eigenvalues of Equation (4) and the original crystalline Schrödinger equation are identical. The following sections will outline how the pseudopotential equation can be solved.

There is no unique solution to Equation (4) since any core-electron eigenstate $|nl\rangle$ may be added to $\phi_{\vec{k}}(\vec{r})$ and the combination will still remain a solution of the pseudopotential equation. If $\phi_{\vec{k}}(\vec{r})$ could be obtained exactly (i.e., to all order of perturbation theory), this non-uniqueness would not matter since any exact solution of $\phi_{\vec{k}}(\vec{r})$ would yield the same conduction eigenstate $\psi_{\vec{k}}(\vec{r})$. This is evident from the relationship between $\psi_{\vec{k}}^C(\vec{r})$ and $\phi_{\vec{k}}(\vec{r})$ shown in Equation (7).

$$\psi_{\vec{k}}^C(\vec{r}) = (1 - P)\phi_{\vec{k}}(\vec{r}) \quad (7)$$

Since $\phi_{\vec{k}}(\vec{r})$ will be obtained to first order in perturbation theory it is necessary to further specify how $\phi_{\vec{k}}(\vec{r})$ can be made unique.

Cohen and Heine (1961) have suggested that an appropriate condition for uniqueness is that the pseudopotential equation should be solved for the 'smoothest' wave function. They impose the criteria that $\phi_{\vec{k}}(\vec{r})$ should minimize the following quantity,

$$\int |\nabla \phi_{\vec{k}}(\vec{r})|^2 d^3r / \int |\phi_{\vec{k}}(\vec{r})|^2 d^3r \quad (8)$$

if it is to be the 'smoothest' wave function. This condition in Equation (8) can be shown (Harrison, 1966) to yield the following equivalent criterion for the smoothest pseudo wave function.

$$\langle nl | W | \phi_{\vec{k}} \rangle = \langle \phi_{\vec{k}} | W | \phi_{\vec{k}} \rangle \langle nl | \phi_{\vec{k}} \rangle / \langle \phi_{\vec{k}} | \phi_{\vec{k}} \rangle \quad (9)$$

Utilizing Equation (9) in Equation (4) leads to the following expression for the pseudopotential

$$W(\vec{r})\phi_{\vec{k}}(\vec{r}) = (1 - P)V^C\phi_{\vec{k}}(\vec{r}) + \frac{\langle \phi_{\vec{k}} | (1-P)V^C | \phi_{\vec{k}} \rangle P\phi_{\vec{k}}(\vec{r})}{\langle \phi_{\vec{k}} | \phi_{\vec{k}} \rangle - \langle \phi_{\vec{k}} | P | \phi_{\vec{k}} \rangle} \quad (10)$$

Equation (10) is the nonlinear optimized pseudopotential [i.e., Equation (10) predicts the smoothest $\phi_{\vec{k}}(\vec{r})$ form of the pseudopotential]. Said otherwise the optimized form of $W(\vec{r})$ will produce a uniquely defined $\phi_{\vec{k}}(\vec{r})$ that will be smoothest in the sense of Equation (8).

It is seen that the optimized pseudopotential in Equation (10) is a nonlinear operator since it depends on $\phi_{\vec{k}}(\vec{r})$. However, it can be shown (Harrison, 1966) that $W(\vec{r})$ may be linearized without affecting the second order perturbation theory results for the eigenvalues $E_{\vec{k}}$. The linear optimized form of $W(\vec{r})$ is,

$$W(\vec{r})\phi_{\vec{k}}(\vec{r}) = (1 - P)V^C\phi_{\vec{k}}(\vec{r}) + \frac{\langle \vec{k} | (1-P)V^C | \vec{k} \rangle}{1 - \langle \vec{k} | P | \vec{k} \rangle} P \phi_{\vec{k}}(\vec{r}) \quad (11)$$

One might also note that the linearized pseudopotential in Equation (11) is non-Hermitian due to the term PV^C . However, the eigenvalues $E_{\vec{k}}$ are not affected by the non-hermiticity of $W(\vec{r})$ until third order or higher terms are reached in perturbation theory (Harrison, 1966).

Perturbation theory predicts that the eigenvalues $E_{\vec{k}}$ are to second order,

$$E_{\vec{k}} = \frac{\hbar^2 k^2}{2m} + \langle \vec{k} | W | \vec{k} \rangle + \sum_{\vec{q}}' \frac{\langle \vec{k} + \vec{q} | W | \vec{k} \rangle \langle \vec{k} | W | \vec{k} + \vec{q} \rangle}{\frac{\hbar^2}{2m} (k^2 - |\vec{k} + \vec{q}|^2)} \quad (12)$$

where the matrix elements of $W(\vec{r})$ have been taken between plane wave states, and the sum over \vec{q} has the term $\vec{q} = 0$ omitted. With a little algebra and noting that $P^2 = P$, and $V^C = H - T$, it can be shown that the diagonal and off-diagonal matrix elements of W are (Harrison, 1966),

$$\langle \vec{k} | W | \vec{k} \rangle = \langle \vec{k} | V^C | \vec{k} \rangle + \sum_{n\ell} \left(\frac{\hbar^2 k^2}{2m} + \langle \vec{k} | V^C | \vec{k} \rangle - E_{n\ell} \right) \frac{\langle \vec{k} | n\ell \rangle \langle n\ell | \vec{k} \rangle}{1 - \langle \vec{k} | P | \vec{k} \rangle} \quad (13)$$

and

$$\begin{aligned}
\langle \vec{k}+\vec{q} | W | \vec{k} \rangle = & \langle \vec{k}+\vec{q} | V^C | \vec{k} \rangle + \sum_{n\ell} \left[\frac{\hbar^2 k^2}{2m} - E_{n\ell} + \langle \vec{k} | V^C | \vec{k} \rangle \right] \langle \vec{k}+\vec{q} | n\ell \rangle \langle n\ell | \vec{k} \rangle + \\
& \sum_{n\ell} \left[\frac{\hbar^2 k^2}{2m} - E_{n\ell} + \langle \vec{k} | V^C | \vec{k} \rangle \right] \langle \vec{k} | n\ell \rangle \langle n\ell | \vec{k} \rangle \langle \vec{k}+\vec{q} | P | \vec{k} \rangle / (1 - \langle \vec{k} | P | \vec{k} \rangle) .
\end{aligned}
\tag{14}$$

Equations (13) and (14) represent the unscreened or bare pseudopotential matrix elements. The matrix elements must be screened before they are used in equation (12). The screening of the pseudopotential is discussed in later sections and in Appendix D.

Factorization of the Pseudopotential

Equations (12), (13) and (14) can be used to evaluate the energy of the conduction electrons to second order in perturbation theory, but this is a difficult task because of the complexity of evaluating the crystalline potential. The problem of computing the conduction-electron energy can be greatly simplified if one makes the assumption that V^C and, subsequently, W can be written as a linear superposition of spherically symmetric potentials centered upon the lattice sites. With this assumption, it is possible to factorize the pseudopotential matrix elements in the following manner:

$$\langle \vec{k}+\vec{q} | W | \vec{k} \rangle = S(\vec{q}) \langle \vec{k}+\vec{q} | w | \vec{k} \rangle , \tag{15}$$

where

$$S(\vec{q}) = 1/N \sum_j \exp(-i\vec{q} \cdot \vec{r}_j) \tag{16}$$

and

$$\langle \vec{k}+\vec{q} | w | \vec{k} \rangle = 1/\Omega_0 \int \exp[-i(\vec{k}+\vec{q}) \cdot \vec{r}] w(\vec{r}) \exp(i\vec{k} \cdot \vec{r}) d^3r . \tag{17}$$

The quantity $S(\vec{q})$ is known as the structure factor, \vec{r}_j is the position of the j 'th lattice site, Ω_0 is the primitive unit cell volume, and $w(r)$ is the pseudopotential associated with one unit cell.

If Equation (15) is substituted into Equation (12) and all occupied \vec{k} states are summed over, one obtains for the second order contribution to the conduction-electron energy

$$E = \sum_{\vec{q}} |S(\vec{q})|^2 F(\vec{q}) \quad (18)$$

$F(\vec{q})$ is the energy wave number characteristic and is explicitly

$$F(|\vec{q}|) = 2\Omega_0 / (2\pi)^3 \int \frac{\langle \vec{k} | w | \vec{k} + \vec{q} \rangle \langle \vec{k} + \vec{q} | w | \vec{k} \rangle d^3k}{\frac{\hbar^2}{2m} (\vec{k}^2 - |\vec{k} + \vec{q}|^2)} - \frac{\Omega_0}{2} n^{sc}(\vec{q}) w^{sc}(\vec{q}) \quad (19)$$

The singularity in the denominator of the first term of Equation (19) can be integrated analytically and, therefore, does not cause any great difficulty when $|\vec{k}| = |\vec{k} + \vec{q}|$.

The second term in Equation (19) is the conduction or screening-electron self-energy which has been subtracted once from the expression of $F(\vec{q})$ because the first term has counted it twice. The quantities $n^{sc}(\vec{q})$ and $w^{sc}(\vec{q})$ are the Fourier transforms of the screening-electron charge density and Coulomb potential, respectively. Equation (18) represents the conduction-electron energy dependence upon the crystal structure. Hence, if the crystal is distorted, the function $S(\vec{q})$ changes and affects the value of the conduction-electron energy predicted by Equation (18). Consequently, Equation (18) is of critical importance in calculating phonon spectra or elastic shear constants which depend upon a knowledge of the distorted lattice energy. Appendices A and B derive the explicit relationship between $F(\vec{q})$ and the phonon spectra and elastic shear constants.

IV. THE CRYSTALLINE POTENTIAL AND THE PSEUDOPOTENTIAL

The derivation of the HFP pseudopotential matrix elements was outlined in the preceding sections. It was also demonstrated in Appendices A and B how the phonon dispersion curves and the elastic shear constants of a solid metal may be calculated once the pseudopotential matrix elements are known. Equations (13) and (14) indicate, however, that there are three things which must first be provided before a numerical evaluation of the HFP pseudopotential matrix elements can be made. They are: 1) the core-electron eigenfunctions $|n\ell\rangle$; 2) the core electron eigenvalues $E_{n\ell}$; and 3) the crystalline potential $V^C(r)$. It is far from a trivial task to obtain any one of these three quantities. Therefore, we shall discuss in some detail the analysis for obtaining $|n\ell\rangle$, $E_{n\ell}$, $V^C(r)$ and the approximations that have been employed.

The Core Electron Eigenstates

Ideally, one would like to use core-electron wave functions and eigenvalues that have been calculated self-consistently for the crystal Hamiltonian. However, this is a formidable if not impossible task, and one must resort to approximate descriptions for the core-electron states in the crystal. In the simple metals like the alkalis where there is very little overlap between adjacent atoms in the crystal, the small core approximation may be utilized. This approximation states that the core-electrons in the crystal are described by the wave functions for the electrons in an isolated atom or ion. A self-consistent field calculation was performed to obtain the wave functions and eigenvalues for an isolated ion. These eigenstates were then used to approximate

the core-electron states in the crystal for the purposes of constructing a first principles pseudopotential. The Herman-Skillman (1963) atomic structure program was used to do the actual numerical computation of the free-ion wave functions. The Herman-Skillman (HS) program performed a self-consistent Hartree-Fock-Slater determination of the ionic wave-functions. One could also do a variational determination of the core states, but the HS self-consistent field approach is more in keeping with the first-principles spirit of our calculations.

The HS program also calculates the free ionic eigenvalues which will be denoted as E_{nl}^{HS} . The core-electron eigenvalues in the crystal, E_{nl} , will have different values because of interactions with the crystal environment. The shift in the core-electrons energy in going from the free ionic to the crystalline state is called the 'core shift' (Lin and Phillips, 1965). As will be shown later, it is important to do an accurate determination of the core shifts when doing HFP pseudopotential calculations. The accuracy of the core shift can significantly affect the calculated phonon dispersion curves, and other lattice dynamical properties.

The Crystalline Potential

The crystalline potential was constructed as a linear sum of spherically symmetric potentials. Each of these spherically symmetric potentials arises from the charge density within a single primitive unit cell. The potential within a primitive unit cell 'seen' by the conduction-electrons consists of: 1) the Coulombic potential of the bare ion, where the ion is composed of a delta function nucleus and the localized core-electron charge density, 2) the exchange interaction

between the core and conduction-electrons; 3) the orthogonalization hole (OH) potential; and 4) the self-consistent screening potential of the conduction-electron gas. The OH and screening potentials both arise from the conduction-electron charge density which is obtained by taking the absolute square of $\psi_k^C(r)$ and summing over all occupied k -states.

Contributions 2, 3 and 4 to V^C are discussed in the next two sections and in Appendices C and D. The ion potential, contribution 1, as previously stated, is constructed from the core-electron eigenstates. The eigenstates yield the core charge density and then, with the aid of Poisson's Equation, one obtains the core potential.

V. APPLICATION OF THE PSEUDOPOTENTIAL TO THE CALCULATION OF PROPERTIES OF THE SOLID ALKALIS

The accuracy of a given pseudopotential may be checked by using it to predict properties of the metal that can be verified experimentally. The elastic shear constants and the phonon spectra are two features that may be readily predicted with the aid of the pseudopotential and compared to experiment. The phonon dispersion curves will be discussed first because they constitute a more rigorous test of the correctness of the energy wave number characteristic. The phonon spectra allows a comparison of a set of curves instead of a single number like the elastic constants. The elastic constants depend on $F(q)$ and its derivatives only at the reciprocal lattice vectors \vec{G} , whereas the phonon frequencies $\omega(q)$ depend on the values of $F(|\vec{G}+\vec{q}|)$. Hence the phonon dispersion curves 'sample' a more extended range of the argument of $F(q)$ and are therefore a more sensitive test of the correctness of $F(q)$.

Appendix A gives a detailed mathematical treatment of the theory of the phonon spectra and how the frequencies $\omega(q)$ are calculated once $F(q)$ has been computed. In this section we present a discussion of the sensitivity of the phonon spectra to certain features of the crystalline potential used in the construction of the pseudopotential. More specifically, we will demonstrate the phonon dependence on the conduction-core exchange interaction, the core-electron states, the conduction-electron gas screening, and the shift of the core-electron eigenvalues, i.e., the core shifts.

Phonon Spectra and the Conduction-Core Exchange Interaction

There are several different approximations available for describing the conduction-core (C-C) exchange interaction. Perhaps the best known approximation is the Slater generalized X_α method which, in the case of a nonuniform charge distribution, becomes the so-called local density approximation (LDA)

$$V_{\text{ex}}^\alpha(\vec{r}) = -3(3/\pi)^{1/3} \alpha n_c^{1/3}(\vec{r}) \quad . \quad (20)$$

In our calculations, $n_c(\vec{r})$ is the computed core-electron number density. The coefficient α is known as the exchange parameter and can assume a range of values. In our analysis, α was chosen to have one of the three possible theoretical values that have some first-principles justification. Slater (1951) originally derived Equation (20) for the case of a free electron gas for which the value of α is 1.0. Kohn and Sham (1965), using a variational technique, derived an expression for the exchange potential that was identical to Slater's, except the value they obtained for α was 2/3. More recently, Lindgren and Schwarz (1972) proposed using values of α between 2/3 and 1.0 which predict total energies for a free atom that are equal to the energy predicted by an exact Hartree-Fock calculation.

A second approximation for the C-C exchange potential was proposed by Lindgren (1971). He suggested an exchange potential given by

$$V_{\text{ex}}^L(\vec{r}) = -3(3/\pi)^{1/3} [n_t^{1/3}(\vec{r}) - n_v^{1/3}(\vec{r})] \quad , \quad (21)$$

where the total electronic density n_t is the sum of the conduction $[n_v(\vec{r})]$ and core-electron densities $[n_c(\vec{r})]$. Lindgren derived V_{ex}^L

by noting that V_{ex}^{α} is more properly applied to the total charge density, and that, if one wishes to study the interelectronic conduction-core exchange, then Equation (21) is the more appropriate form for describing this interaction. Note that the exchange potentials in Equations (20) and (21) are quite similar in the core region where $n_c \gg n_v$, but that V_{ex}^L goes to zero much faster in the region where $n_c < n_v$. Therefore, the Lindgren exchange potential predicts a weaker exchange interaction at large r where $n_c < n_v$ than does the Slater, Kohn-Sham, or Lindgren-Schwarz potentials.

It is possible, by adjusting the value of α in Equation (20) or by introducing a parameter α in Equation (21), to fit the calculated phonon spectra to the experimental data. This is due to the fact that changing the value of α in a pseudopotential calculation produces a shift in the magnitude of the calculated frequencies without changing the qualitative shape of the curves. However, the temptation to parameterize α has been resisted because it obscures the significance of other contributions to the pseudopotential (e.g., such as the choice of dielectric screening function). Since our goal of a first principles pseudopotential calculation was to try to elucidate knowledge about fundamental interactions in the solid, all calculations in this thesis utilized one of the conduction-core exchange schemes that had some a priori justification (e.g., Kohn-Sham, Slater, Lindgren, and Lindgren and Schwarz).

To illustrate the sensitivity of the phonon spectra to the choice of conduction-core exchange approximation, we show in Figure 1 two phonon dispersion curves for Li that were calculated using identical pseudopotentials except for the choice of C-C exchange potential. The solid

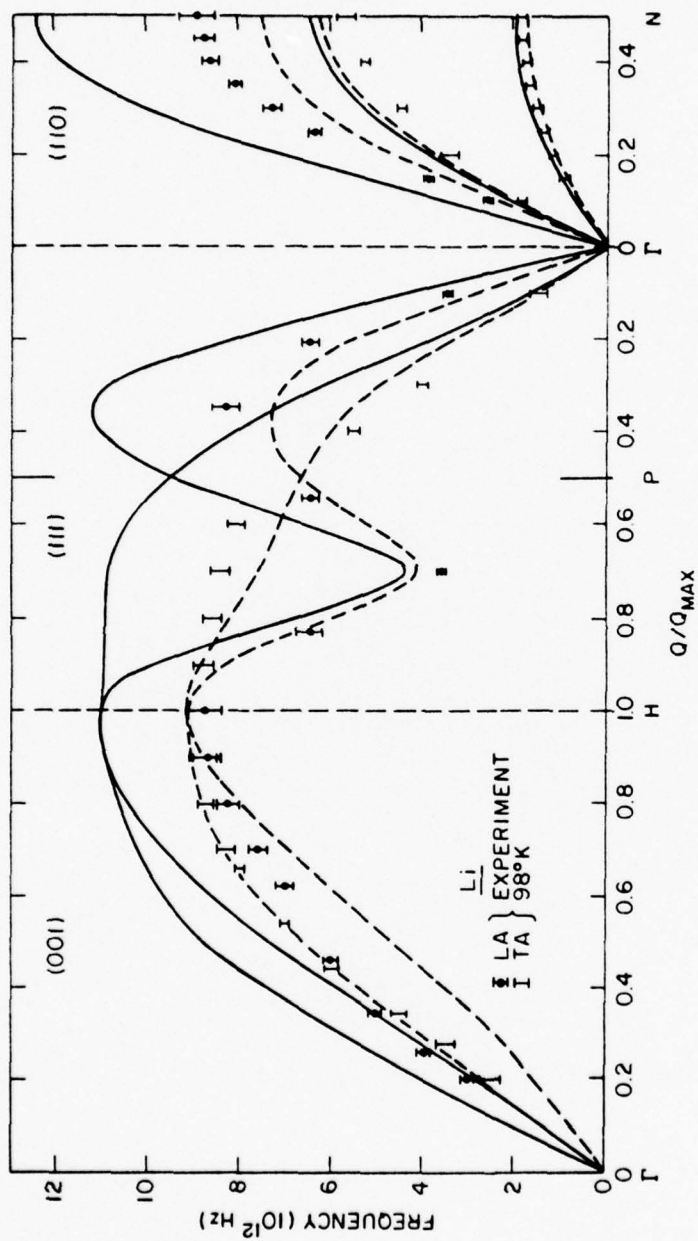


Figure 1. Li phonon spectra showing sensitivity to the conduction-core exchange approximation. Solid curve is computed with Lindgren's exchange approximation, and dashed curve with the Kohn-Sham approximation. Data points are from Smith et al. (1968).

curve employed V_{ex}^L , and the dashed curve used V_{ex}^α with Kohn and Sham's value for α . The curves are chosen only to illustrate the dramatic differences produced in the phonon spectra by different treatments of the conduction-core exchange, and were not chosen to represent the best agreement with experiment. The dashed curve would have been even lower if Slater's α was used for V_{ex}^α . Na, K, Rb and metals, such as the hcp divalent series, show similar sensitivity to the conduction-core exchange.

It is possible to make some general observations concerning the conduction-core exchange approximations of Equations (20) and (21). In general it was found that V_{ex}^α of Equation (20) predicted phonon frequencies for Na and K that had the longitudinal acoustic (LA) and transverse acoustic (TA) branches in the (001) direction inverted with respect to experiment. The inversion of the LA and TA modes in the (001) direction was not corrected by the use of different dielectric screening functions, and seems to be a symptom of V_{ex}^α . We note that in the other crystal directions, (110), (111), where the LA and TA modes are not so nearly degenerate, V_{ex}^α produces good agreement with experiment, with the LA and TA branches properly ordered. On the other hand, the Lindgren exchange approximation, Equation (21), does predict the LA and TA branches in the correct order for the (001) direction of Na and K. Hence, for Na and K, the Lindgren potential V_{ex}^L is preferable to V_{ex}^α because it predicts the correct ordering of the phonon modes in the (001) direction, as well as yielding better qualitative agreement.

There is another reason why V_{ex}^L is preferable to V_{ex}^α when calculating phonon frequencies for Na and K. Lindgren exchange, V_{ex}^L

appears more compatible with the dielectric screening functions which go beyond the Hartree approximation. The use of V_{ex}^{α} in conjunction with the Hartree free electron gas dielectric function (Sham and Ziman, 1963) predicts phonon frequencies in good agreement with experiment (except for the mode inversion). However, when the interacting electron gas dielectric functions are used with V_{ex}^{α} or V_{ex}^L , the LA phonon frequencies are lowered. This improves agreement with experiment if V_{ex}^L is used, but further aggravates the mode inversion of the (001) LA and TA branches which occurs with V_{ex}^{α} . The dielectric function of Singwi, et al. (1970) (SSTL) is an example of an interacting electron gas screening function that produces this sort of behavior.

Although V_{ex}^L definitely produces better phonon spectra for Na and K than does V_{ex}^{α} , the same cannot be said for Li. V_{ex}^L yields phonon frequencies for Li that are much too high in comparison to experimental results, regardless of the dielectric screening function that was employed. When V_{ex}^{α} is used with the Hartree dielectric function one obtains phonon frequencies for Li which are in quite good agreement with experiment (see, for example, Figure 6). Furthermore, the cross over of the La and Ta branches in the (001) direction of Li is correctly predicted. In the calculations presented here, the quantity $n_v(r)$ in V_{ex}^L was approximated by $1/\Omega_0$, the uniform conduction-electron density. Recent calculations by Sun (1978) show that by approximating $n_v(r)$ in V_{ex}^L by the more accurate single OPW density [i.e., $n_v(r) = z^*/\Omega_0 + n^{OH}(r)$], the phonon curves for Li were slightly lowered. Though this was still not enough to produce good agreement with experiment, it may indicate that V_{ex}^L would work for Li if

n_v was known sufficiently accurately. Sun also used the single OPW result for n_v in calculations for Na, K, and Rb and found that, in all cases, the more rigorous treatment of n_v in V_{ex}^L improved agreement with experimental phonon curves.

Phonon Spectra and the Core-Electron Eigenstates

In the HFP pseudopotential formalism, the core-electrons are represented by either an analytic or numerically computed wave function. This sets the HFP formalism apart from model pseudopotential calculations which do not explicitly include core-electron states in the construction of the pseudopotential. The Herman-Skillman (1963) atomic structure program was used to calculate the ionic eigenvalues (E_{nl}^{HS}), and the radial part of the core-electron wave function $P_{nl}(r)$ for the ion in the free state. The HS program is a self-consistent field calculation based upon a Hartree-Fock-Slater formalism.

There are several aspects of the HS program that deserve some attention. The first point is that the core-electron states can be calculated with different approximations for the exchange interaction among the core-electrons. It was found that the phonon spectra were significantly affected by the use of different exchange approximations in the HS core state calculation. In Figure 2, there are two phonon dispersion curves for K that were calculated with identical pseudopotentials except that the solid curve used core states calculated with Slaters exchange [i.e., Equation (20) with α equal to 1] and the dashed curve used core states calculated with Lindgren and Schwarz's value for the α -parameter [Equation (20) with α equal to 0.722]. As can be seen, there is a very significant difference in the two curves. It is tempting to conclude

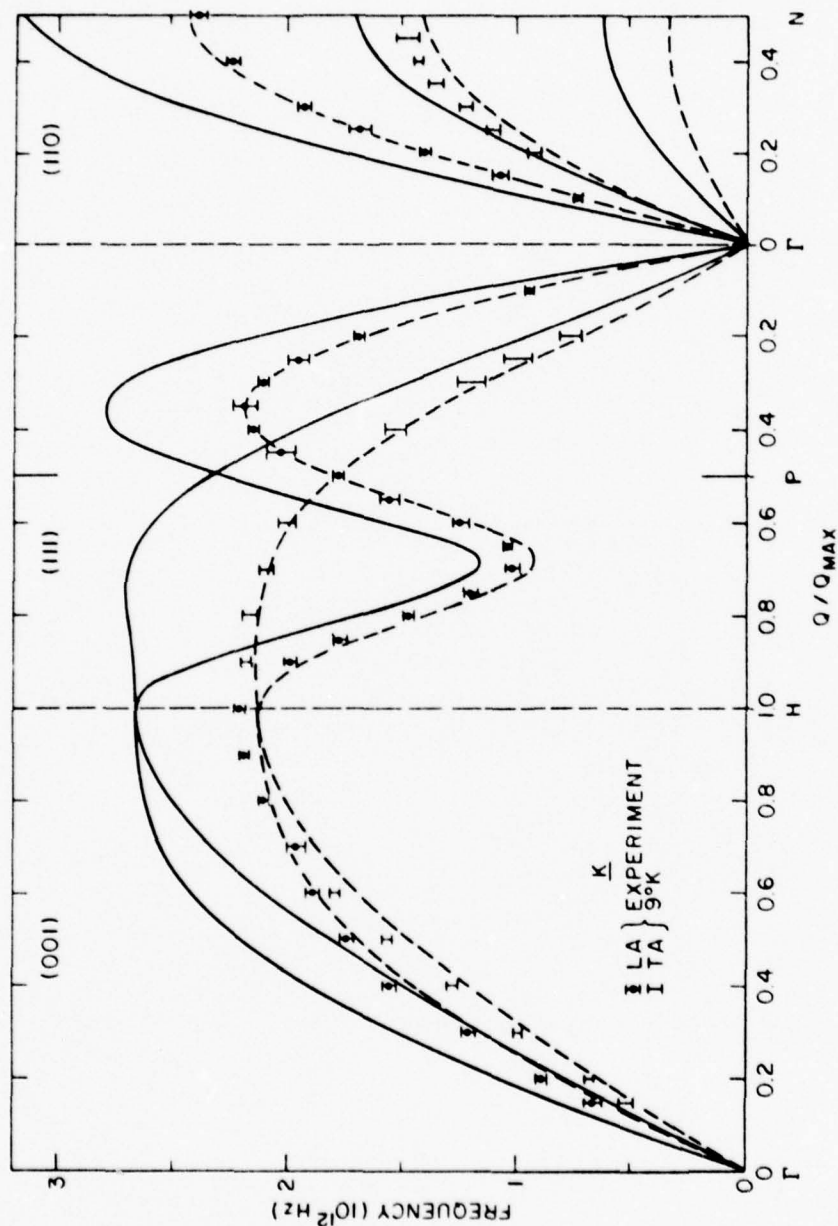


Figure 2. Sensitivity of the phonon spectra of K to the exchange approximation used in the construction of the core-electron states. Both curves were computed from identical pseudopotentials except the solid curve resulted from core states calculated with Slater's exchange approximation [$\alpha = 1.0$ in Equation (20)] and the dashed curve from Lindgren and Schwarz/ approximation [$\alpha = 0.722$ in Equation (20)]. Experimental data points for K are from Cowley et al. (1966).

on the basis of Figure 2 that the Lindgren and Schwarz exchange approximation provides a better description of the core-electron states, but as we shall see, this is not necessarily so. Further study of the effect of the exchange approximation upon the core states reveals that Slater's approximation yields core state eigenvalues that are in better agreement with experiment than eigenvalues predicted by any of the other exchange approximations previously discussed. Therefore, using as a criterion the difference between the experimental and theoretical eigenvalues, one finds that Slater's approximation for the exchange interaction is the most appropriate choice for the core wave function calculation. Thus, the apparently excellent agreement in Figure 2 predicted by the Lindgren and Schwarz core states may be partly fortuitous.

Although the use of Slater's exchange in the construction of the HS core states gives best agreement between experimental and theoretical core eigenvalues, differences that remain are still significant. Day et al. (1976) showed for Li and Be that the differences between the theoretical and experimental core eigenvalues could measurably affect the resulting theoretical phonon dispersion curves. Figure 3 illustrates, for Li, the differences in the phonon spectra produced when theoretical and experimental core eigenvalues are used. In principle, the experimental ionic eigenvalues (with appropriate core shifts) should always be used in HFP pseudopotential calculations, but for multi-orbital cores like Na and K, there is little reliable spectroscopic data available for the ion. Theoretical term values were employed in our calculations due to the unavailability of experimental data for the inner shell ionic energy levels. Table 1 lists experimental and theoretical eigenvalues for the Li ion and the Na and K atoms [Slater (1955), Bearden and Burr (1967), CRC Handbook (1972)].

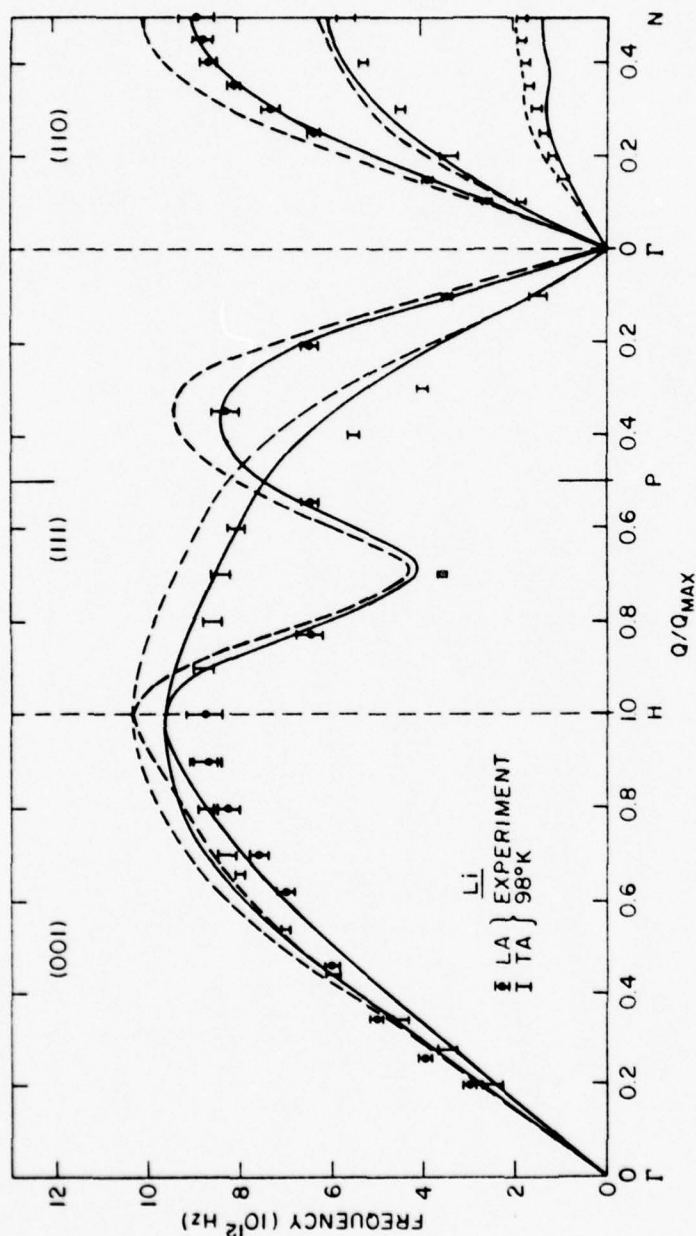


Figure 3. Demonstration of phonon spectra sensitivity to the core-electron eigenvalue E_{nl} . The dashed curve is calculated using the experimental eigenvalue while the solid curve used a theoretically determined eigenvalue. Experimental points for Li are from Smith et al. (1968).

Table 1. Experimental versus theoretical eigenvalues for the Li^+ ion and the Na and K atoms.

E_{nl}	Experiment (Rydbergs)	Theory (Rydbergs)
Li^+_{1s}	- 5.56	- 5.38
Na_{1s}	- 79.4	- 78.0
2s	- 5.2	- 4.7
2p	- 2.8	- 2.67
3s	- 0.38	- 0.37
K_{1s}	-266.2	-262.1
2s	- 28.2	- 27.1
2p	- 22.2	- 22.0
3s	- 3.0	- 2.95
3p	- 1.81	- 1.73
4s	- 0.32	- 0.308

The Conduction-Electron Potential and the Phonon Spectra

The conduction-electron charge density is, for convenience, separated into two different parts, the orthogonalization hole density $n^{\text{OH}}(\vec{r})$ and the screening charge density $n^{\text{sc}}(\vec{r})$. The density $n^{\text{OH}}(\vec{r})$ is independent of the perturbing potential $W(\vec{r})$ and is the result of orthogonalizing the plane-waves to the core wave functions. The screening charge represents the linear response of the conduction-electron gas to $W(\vec{r})$. These charge densities each give rise to their own respective potentials which are important contributions to the crystalline potential. They also interact with the core-electron charge density which produces a shift in the eigenvalues of the core-states. The core shift due to n^{OH} has been given the special name v^{OPW} .

Cutler et al. (1975) and Sun et al. (1976) have shown in calculations of phonon spectra that it is important to do an 'exact' treatment of $n^{\text{OH}}(\vec{r})$ and v^{OPW} , instead of the approximate treatments proposed and used

by Harrison (1966). A detailed derivation and discussion of the exact and approximate OH treatments is presented in Appendix C. Moriarty (1970) has used an exact treatment of the OH for the noble metals Cu, Ag, and Au but the calculations in this thesis are the first to use an exact n^{OH} for the alkali metals.

The effect of the exact treatments of n^{OH} and v^{opw} is seen in Figure 4 where the phonon spectra for Li calculated with the exact OH (solid curves) is compared with a similar calculation, using, however, an approximate OH (dashed curves). The effect of the exact n^{OH} is to significantly lower (i.e., by 5 to 10% at the Brillouin zone boundaries) the phonon dispersion frequencies. Similar behavior is noted for Na and K.

A derivation of the screening potential w^{SC} is given in Appendix D, where it is pointed out that the screening of the conduction-electron gas can be described by a scalar or static dielectric response function $\epsilon^*(q)$.

$$\epsilon^*(q) = 1 + (1 - \epsilon(q))(1 - G(q)) \quad . \quad (22)$$

The function $\epsilon(q)$ is the free-electron or Hartree dielectric function [see Equation (D.10)] and $G(q)$ is a function which accounts for the effects of electronic exchange and correlation between the conduction electrons. For a free-electron gas, $G(q)$ is zero and $\epsilon^*(q)$ becomes equal to $\epsilon(q)$. Although there is no exact solution for $G(q)$ for an interacting system, there have been many attempts at calculating approximate forms for this exchange-correlation function [Toigo and Woodruff (1971), Geldart and Taylor (1970), Hedin and Lundqvist (1971)].

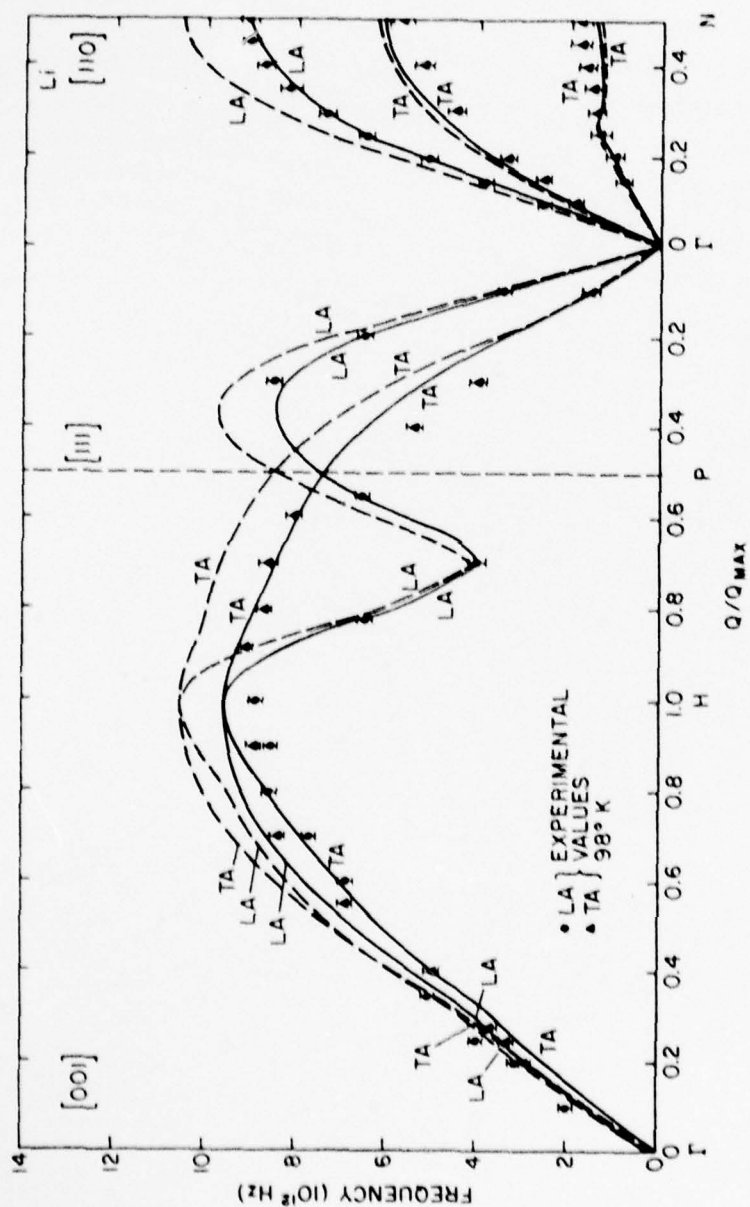


Figure 4. Exact versus approximate treatment of the orthogonalization hole and its influence upon the Li phonon spectra. Approximate treatment (dashed curve) and exact treatment (solid curve) are compared to the experimental data of Smith et al. (1968).

For a number of reasons the $G(q)$ of Singwi et al. (SSTL) (1970) was employed in most of our calculations. Firstly, the SSTL evaluation of $G(q)$ can be represented by the simple analytic expression of Equation (23)

$$G(q) = A \left[1 - e^{-Bq^2/k_F^2} \right], \quad (23)$$

which is convenient for use in numerical calculations. Secondly the dielectric function must satisfy certain relations involving the pair correlation function $g(r)$ for $r \rightarrow 0$ and the isothermal compressibility (the inverse of the bulk modulus) SSTL (1970). The SSTL dielectric function makes reasonable predictions for $g(r)$ at small r and closely satisfies the so-called compressibility sum rule. The limiting values of $G(q)$ go from zero at small q to ≈ 1 at large q , i.e., $q \geq 2k_F$.

Figure 5 shows two sets of phonon spectra for Na that were calculated with identical pseudopotentials except that the dashed curve employed the SSTL $G(q)$ and the solid curve was calculated with the Hartree $\epsilon(q)$, i.e., $G(q) = 0$. Significant differences are observed in the two sets of phonon spectra, though not as significant as those that are produced by different treatments of the conduction-core exchange interaction or the core-electron states. The effect of non-zero $G(q)$ dielectrics is to reduce the LA phonon frequencies with respect to those predicted by the Hartree dielectric function. As one would expect, the TA frequencies are not as strongly influenced by the dielectric screening function. Our calculations indicate that the specific form of $G(q)$ is not critically important; however, it is important to include some form of the exchange-correlation screening in the calculations.

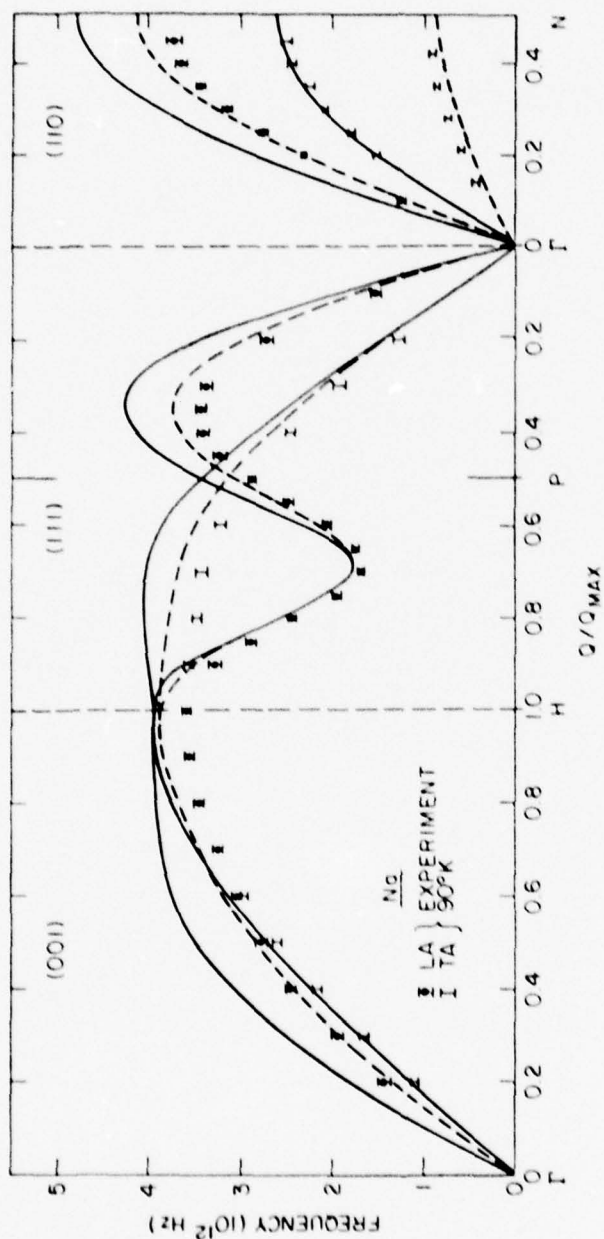


Figure 5. Phonon spectra for Na calculated with the Hartree and SSTL dielectric screening functions. The solid curve resulted from Hartree screening and the dashed curve from the SSTL description of screening. Experimental points are from Wood et al. (1962).

VI. PHONON SPECTRA AND ELASTIC SHEAR CONSTANTS OF THE SOLID ALKALI METALS

Results for Li, Na and K

In the previous sections, it was shown how an HFP pseudopotential is formulated and how the crystalline potential can be constructed. In addition, the dependence of the phonon spectra on various contributions to the crystalline potential was demonstrated. More specifically, we considered the dependence of the crystalline potential on the conduction-core exchange interaction, and the dielectric screening of the conduction electron gas. Pseudopotentials were calculated for Li, Na, and K using various combinations of the conduction-core exchange potential (i.e., V_{ex}^L or, V_{ex}^α with one of the possible a priori values of α) and the dielectric screening function (i.e., the Hartree or SSTL dielectric functions). The validity of each pseudopotential was tested by calculating the phonon spectra, elastic shear constants and the ion-ion pair potentials. In this section the results of these calculations will be presented.

All pseudopotentials that were tested included an exact treatment of the OH density. The core-electron states were calculated by the HS atomic structure program which has been discussed previously in Sections IV and V. For Na and K, it was found that a combination of Lindgren's exchange potential and the SSTL dielectric screening function in the pseudopotential gave the best overall agreement with experimental phonon spectra and elastic shear constants. On the other hand, the best results for Li were obtained with the Kohn-Sham description of the conduction core exchange and the Hartree dielectric function for the conduction electron gas. The phonon spectra predicted by these pseudopotentials

for Li, Na and K are shown in Figures 6, 7 and 8, respectively. Table 2 lists the elastic shear constants for Li, Na and K predicted by these same pseudopotentials. The details of the elastic shear constant calculation for these BCC materials are given in Appendix B. For the latter, theoretical results are generally within 20% or better of the experimental data.

These results can be considered as quite good when one remembers the fundamental nature of the a priori pseudopotential calculations. It is worth noting that we have also studied one parameter schemes which produce pseudopotentials that yield nearly perfect agreement with experimental phonon spectra and elastic shear constants. However, the use of the a priori approach is capable of producing insight into some of the fundamental interactions in the solid which the model or parameterized pseudopotential cannot, in general, do. It is encouraging to note that the best results for Na and K were obtained with consistent treatments of the conduction core exchange interaction and conduction gas screening. In these calculations for Na, and K, the conduction electron density $n_v(r)$ in Equation (21) for Lindgren's exchange was approximated by the average plane wave density $1/\Omega_0$. Sun (1978) has shown that by approximating $n_v(r)$ by the 1-OPW density, the phonon spectra for Na and K are brought into almost perfect agreement with experiment. He also obtained similar excellent results for the heavier alkali metal Rb. This reinforces the evidence that Lindgren's C-C exchange approximation is a good description for the alkalis. It is disappointing but not really surprising that the pseudopotential for Li required a different treatment of these same interactions. Ham (1972), in his classic calculations of the band

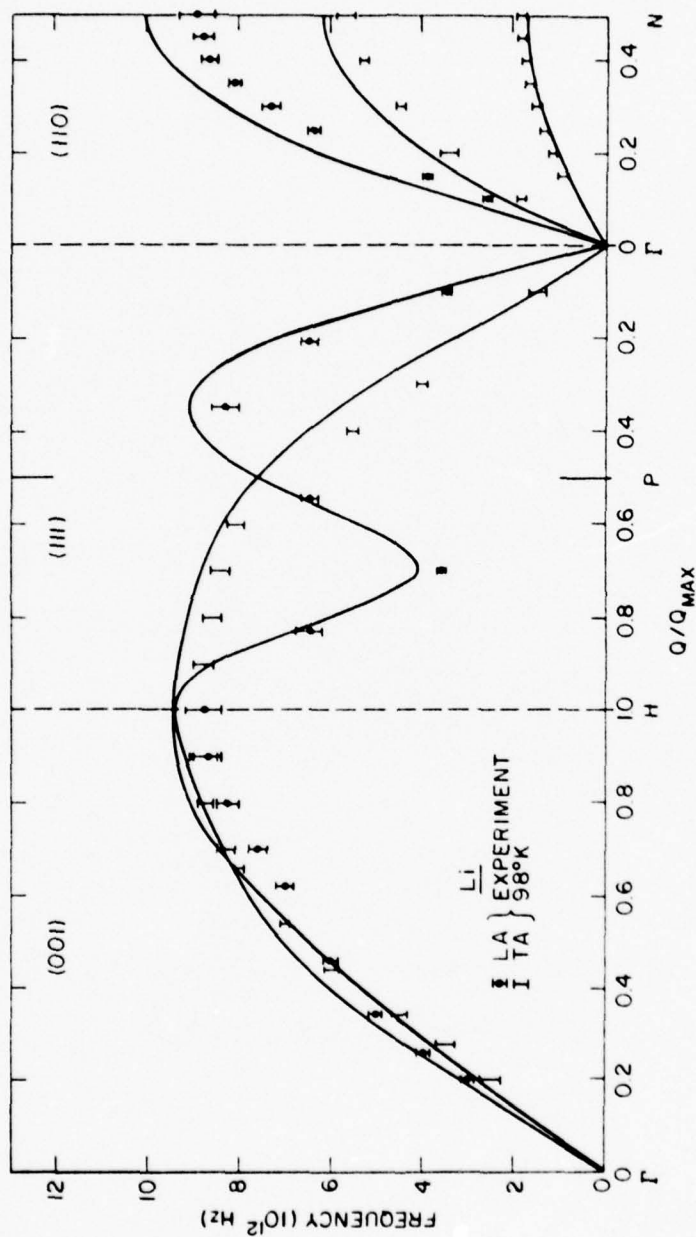


Figure 6. Phonon spectra for Li using a Kohn-Sham treatment of the conduction-core exchange and a Hartree dielectric screening function. Experimental data of Smith et al. (1968).

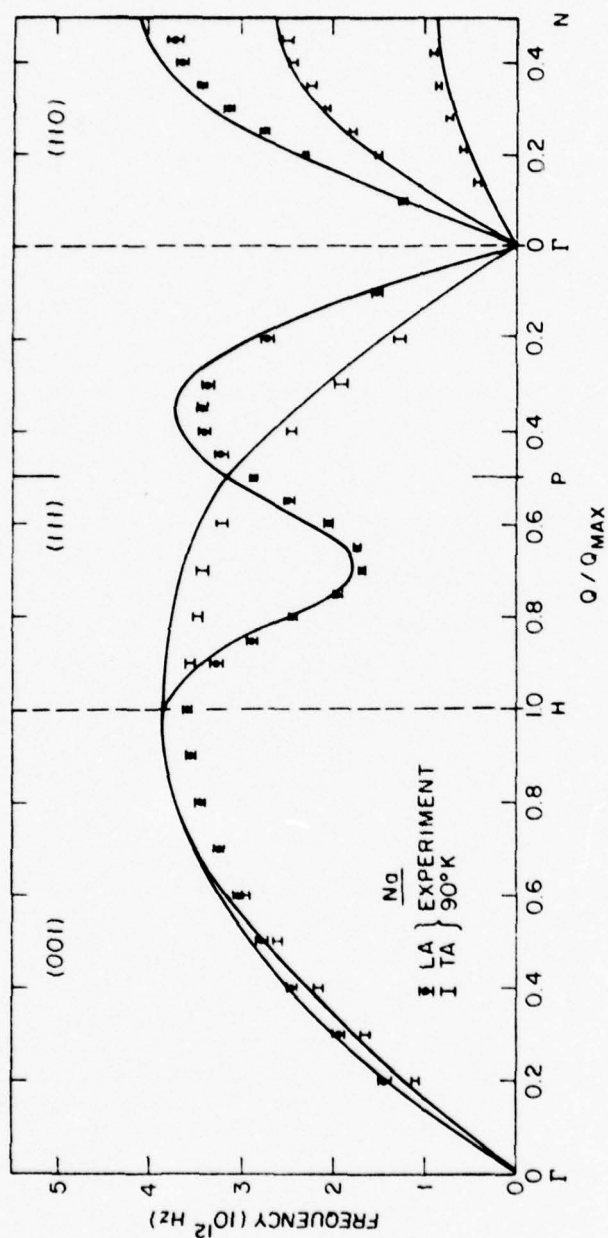


Figure 7. Phonon spectra for Na using Lindgren's approximation to the conduction-core exchange and Singwi et al.'s (1970) dielectric function. Experimental points are from Wood et al. (1962).

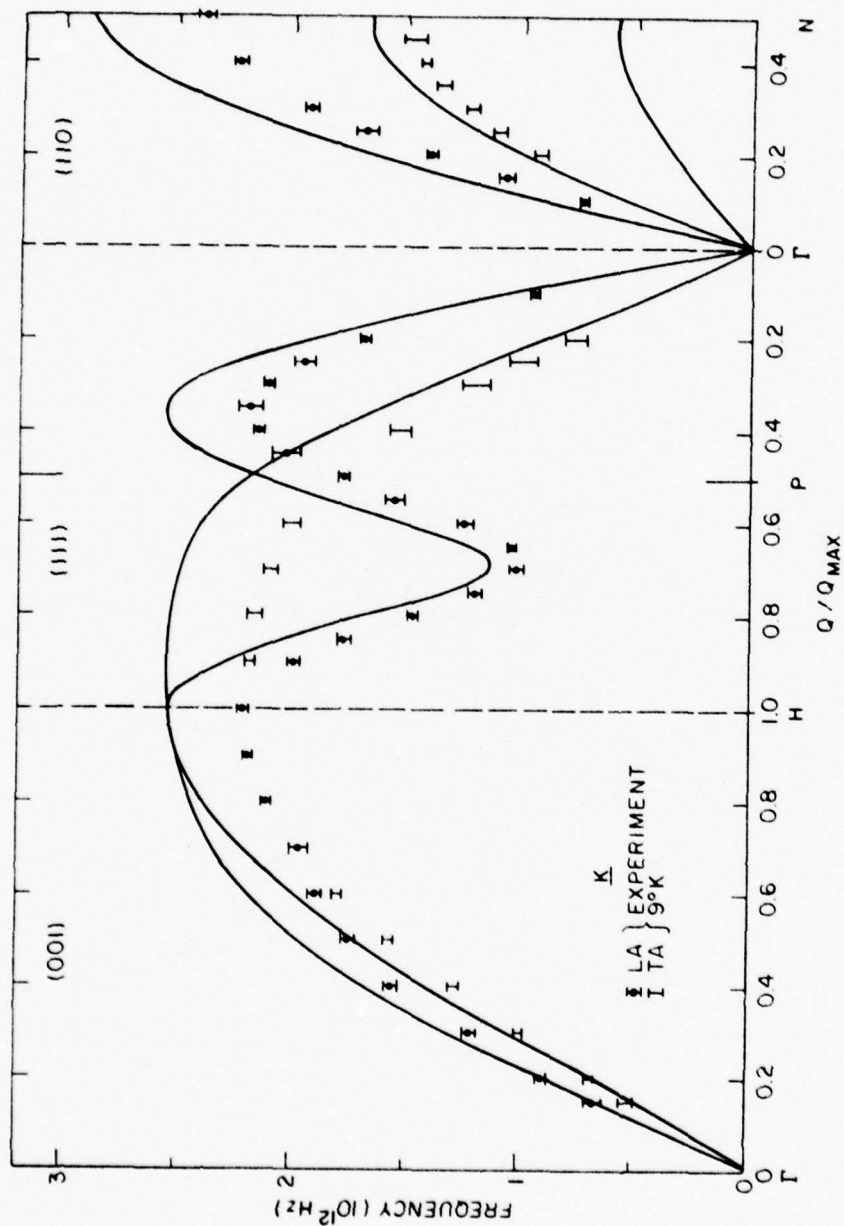


Figure 8. Phonon spectra for K from a pseudopotential using Lindgren's approximation to the conduction core exchange and Singwi et al.'s (1970) dielectric screening function. Experimental points are from Cowley et al. (1966).

Table 2. Elastic shear constants for the simple alkalis Li, Na, and K.
Units of 10^{12} dyne/cm².

		C_{44}	$C_{11}-C_{12}$
Li	exp	0.108	0.0230
	th	0.126	0.0187
Na	exp	0.0577	0.0138
	th	0.0631	0.0137
K	exp	0.0286	0.0075
	th	0.0355	0.0080

structure for the alkali metals found that Li has the greatest relative deviation from free electron like behavior. When Lindgren exchange was used for Li, it was found that the phonon frequencies were raised much too high regardless of what dielectric function was used. Although we have obtained pseudopotentials for all the simple alkalies which yield reliable results for the solid state and Sun has shown how refinements may be made, the anomalous behavior of Li suggests that as of yet there exists no single unified description for constructing the pseudopotential of simple metals.

VII. CALCULATION OF THE LIQUID METAL PROPERTIES OF THE ALKALIS

It has been shown in the preceding sections that a first principles non-local pseudopotential can reliably predict properties of simple metals, such as the alkalis, in the solid state. This was demonstrated explicitly for the elastic shear constants and phonon spectra of Li, Na, and K. We will now show that it is possible to predict properties of the liquid alkali metals using a first principles pseudopotential with appropriate modifications for the liquid state.

Liquid Metal Structure

Before determining the structure of liquid Li, Na, and K using pair potentials that are obtained from a pseudopotential calculation, a brief discussion of what is meant by 'liquid structure' will be presented.

The concept of structure obviously has different implications in liquid and solid systems. The particles in a solid have definite lattice positions, but in a liquid the particles are not locked into definite locations and are much freer to move about than in a solid. The motion and positions of the particles in the liquid will be correlated because of the interactions between the particles. Hence when one says a liquid has structure, one implies that there is correlated behavior of the particles in the liquid and not that there is a rigid lattice structure.

Perhaps the most direct way to recognize that there is structure in a liquid system is to observe the results of an X-ray or neutron

diffraction experiment performed upon a real liquid, and contrast this with the ideal liquid and ideal crystal cases. In any diffraction experiment, the object is to obtain the diffracted intensity $I(\theta)$ of X-rays or neutrons as a function of the scattering angle θ . For an ideal crystal with perfect ordering, the diffracted intensity I is zero except at a finite number of angles where sharp spikes occur in the intensity of the diffracted X-rays or neutrons (see Figure 9). This is the well known Ewald sphere scattering which is discussed in any elementary solid state physics text [e.g., Ziman (1972)]. Consider now an ideal liquid which has perfect disorder. In the ideal liquid, there is no correlation between the positions of the particles and it can therefore be considered to be a homogeneous continuum. The diffracted intensity will show no angular dependence because all angles of scattering are equally likely for this ideal limit. The ideal liquid would display a perfectly uniform diffracted intensity, as is illustrated in Figure 9. On the other hand, $I(\theta)$ for a real liquid does show a definite angular dependence that lies somewhere between the discrete angle scattering of the ideal crystal and the diffuse scattering of the ideal liquid as Figure 15 illustrates.

One can obtain from experimental diffraction experiments a function $S(q)$ known as the interference function or the structure factor. $S(q)$ is proportional to the square of the diffracted intensity and q is the wavenumber of the diffracted radiation which is related to the scattering angle (March, 1966). $S(q)$ can also be calculated theoretically. The formal definition of $S(q)$ is given by

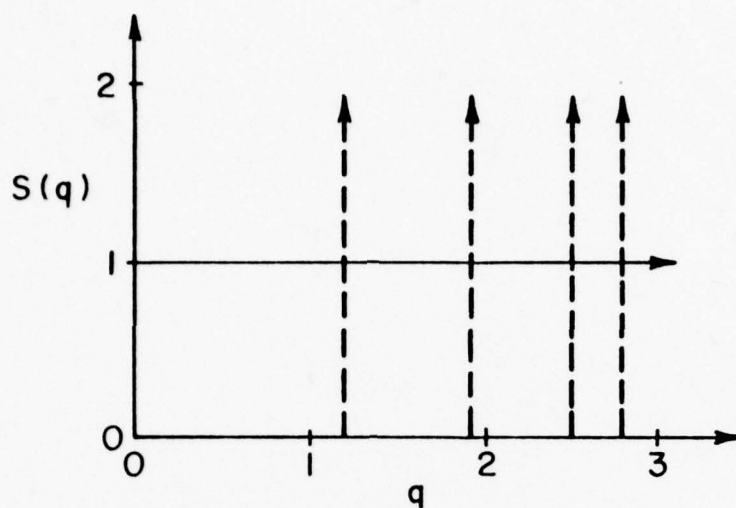


Figure 9. Structure factor, $S(q)$, curves for ideal systems. Solid curve - liquid system, dashed curve - ideal crystal. $S(q)$ is proportional to the square of the diffracted intensity.

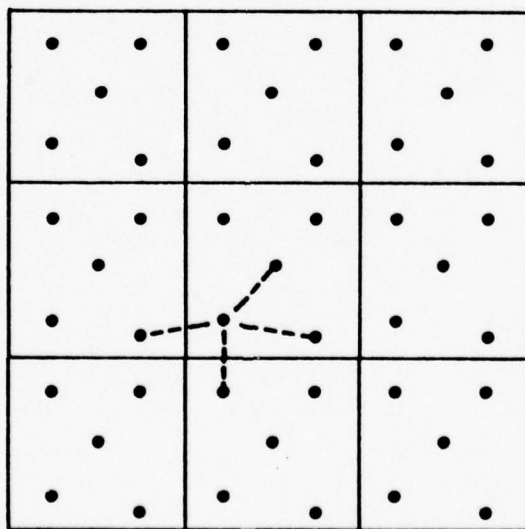


Figure 10. Model of a two-dimensional liquid with $N = 5$ particles per cell and periodic boundary conditions. Each particle is allowed to interact with its $N-1$ nearest neighbors.

$$S(\vec{q}) = 1/N \overline{\sum_{i,j} \exp [i\vec{q} \cdot (\vec{r}_i - \vec{r}_j)]} \quad , \quad (26)$$

where the i, j sum is over the coordinates of the N particles and the bar denotes that an ensemble or configurational average is to be taken (Faber, 1972).

Another manner in which the liquid structure can be specified is through a hierarchy of correlation functions (Croxtan, 1974). In general one may define 2, 3, ..., N -body correlation functions which completely specify the liquid structure if all are known. The two-body correlation function $g(r)$ is also known as the pair correlation or radial distribution function. The function $g(r)$ represents the probability density that a pair of particles in the liquid are a distance $|\vec{r}|$ apart. If one particle is at the origin, then the probability that a second particle is in d^3r about r is $n_0 g(r) d^3r$, where n_0 is the average number density. The pair correlation function is of particular interest because it and $S(q)$ form a Fourier transform pair:

$$S(\vec{q}) - 1 = n_0 \int (g(\vec{r}) - 1) \exp (i\vec{q} \cdot \vec{r}) d^3r \quad . \quad (27)$$

To be more precise, $S(\vec{q}) - 1$ and $g(\vec{r}) - 1$ constitute the Fourier transform pair.

Closely related to $g(r)$ is the cumulative distribution function $G(r)$. This function represents the total number of neighbors within a distance r of a particle located at the origin $r = 0$. In terms of the pair correlation function, $G(r)$ is

$$G(r) = 4\pi n_0 \int_0^r g(r') r'^2 dr' \quad . \quad (28)$$

$G(r)$ and $g(r)$ specify how pairs of particles are distributed in the liquid, and in general they are related to three-body and higher correlation functions; these will not be discussed in this work.

Having defined the meaning of 'liquid structure,' one is now confronted with the task of determining that structure. The interactions between the particles of a liquid are responsible for its structure. If the particles in the liquid are assumed to interact via a spherically symmetric two-body pair potential $U(r)$, then the energy of the j 'th particle interacting with its neighbors in an N particle system is

$$E_j = \sum_{i \neq j}^N U(|\vec{r}_i - \vec{r}_j|) \quad . \quad (29)$$

The effective ion-ion pair potential $U(r)$ can be calculated from pseudopotential theory and will be discussed in detail later.

Methods for Calculating the Liquid Structure

There are a number of theories which relate the potential $U(r)$ to the liquid structure. Perhaps the best known of those which have had some success in the past are the Percus-Yevick (1958) and the Born-Green (1946) theories. However, there are much more direct and reliable approaches to the calculation of the liquid structure. These are the Monte Carlo (MC) and Molecular Dynamics (MD) computer simulations. The MC and MD methods use the computer to simulate the actual behavior in the liquid system. In the MD method, one solves the equations of motion for N particles in a box with periodic boundary conditions. After some assumptions have been made for the

particle's initial positions and velocities, their subsequent trajectories can be computed if the interaction potential $U(r)$ is known. In the MD method, the computer records the particles coordinates as time progresses and computes a time average of whatever property of the system is of interest. On the other hand, the Monte Carlo method computes an ensemble average value of $f(x)$, where $f(x)$ can be any static property of the liquid such as its structure. In the MC calculation, the computer generates random configurations of the N particles and calculates the relative probability of each configuration's occurrence. The ensemble average value of $f(x)$ is formed by calculating its configuration weighted average. The next few sections will discuss the details of this process.

The Monte Carlo Calculation and the Markov Chain

The Monte Carlo technique can be used to estimate the ensemble or configurational averages. If $\vec{x} = (\vec{r}_1, \vec{r}_2, \dots, \vec{r}_N)$ is the N -body collective coordinate for a system of N interacting particles confined to a volume Ω , and $f(\vec{x})$ is any non-singular reasonable function of \vec{x} , then the petit-canonical ensemble average value of $f(\vec{x})$ is

$$\bar{f} = \frac{\int f(\vec{x}) \exp [-\beta U_N(\vec{x})] d^{3N}x}{\int \exp [-\beta U_N(\vec{x})] d^{3N}x}, \quad (30)$$

where $U_N(\vec{x})$ is the interaction potential between the N particles, and β is the usual Boltzmann factor $1/kT$. As is well known, the $3N$ dimensional integrals in Equation (30) have analytic evaluations for

only a very small class of $U_N(\vec{x})$ and $f(\vec{x})$. Therefore, it is in general necessary to have a method of approximating Equation (30) for arbitrary U and f . The Monte Carlo method calculates the ensemble average value of $f(\vec{x})$ by using the following expression

$$\bar{f} = 1/N_c \sum_{i=1}^{N_c} f(x_i) . \quad (31)$$

The sum in Equation (31) is over possible configurations x_i that the coordinates of the N particles may assume, and N_c is the total number of configurations included in the sum. The prime on the sum denotes that the configurations x_i included in the sum were chosen in a particular way to constitute a so-called 'Markov Chain.' Choosing the set of configurations $\{x_i\}_{i=1}^{N_c}$ so that they constitute a Markov Chain ensures that each x_i enters the sum in Equation (31) with its relative probability of occurrence. Therefore Equation (31) represents a simple weighted average. The above discussion, although brief, sums up the essence of the MC technique. A more detailed discussion is given in Metropolis (1953) or Wood (1968).

The liquid structure of the alkali metals was determined using the Monte Carlo method. Since this method is basically a computer simulation technique, a model of the liquid had first to be established. The liquid metal system was represented as a cube of side L containing N particles. The values of N and L were chosen so that N/L^3 equalled the average number density of the liquid system being studied. The number of particles in the cube was chosen arbitrarily as either 125 or 216. Surface effects for small systems of this size could

appreciably affect the structure. To limit the effect of the surface upon the structure and to simulate an infinite system, periodic boundary conditions were employed. Hence, if a particle in the box moved out through one face of the cube, an identical particle would enter the opposite face. The particles in the cube interacted with each other and with particles in adjoining cubes (adjoining cubes due to periodic boundary conditions) via an effective ion-ion pair potential $U(r)$. As previously mentioned, $U(r)$ was calculated using first principles pseudopotential theory. A two-dimensional analog of this three-dimensional system is illustrated in Figure 10 with only five particles in each cell for the sake of simplicity.

The generation of the configurations constituting the Markov Chain was accomplished by randomly moving the particles in the cube one at a time. The move of a particle was accomplished with the aid of a random number generator. Three random numbers were used to change the x, y , and z coordinates of a particle every time it was moved. Each time a particle was moved, a test was performed to determine whether the new configuration would be retained as a member of the Markov Chain or whether it would be rejected and the original configuration would be recounted as a member.

The exact method for testing whether a configuration will be accepted or rejected as a Markov Chain member proceeds as follows. A particle is moved from its initial position to a trial position. The energies E^i and E^t are calculated for the particle in its initial and trial positions, respectively. These energies are then used to

calculate the Boltzmann probability factors P^i and P^t corresponding to the initial and trial positions, where P is given by

$$P = \exp (-E/k_B T) \quad . \quad (32)$$

The energies E^i and E^t are computed by using Equation (29) to sum over the $N-1$ nearest neighbor pair interactions. The inclusion of the $N-1$ nearest neighbors in the energy sum is known as the 'minimum image convention' and is illustrated for the two-dimensional system of Figure 10 (Wood and Parker, 1957). When $P^t \geq P^i$, the trial configuration is automatically accepted as a member of the Markov Chain and it becomes the initial configuration the next time a particle is moved. However, if $P^i > P^t$, then the ratio P^t/P^i is formed and a random number $0 \leq R \leq 1$ is also generated. If $P^t/P^i \geq R$, then the trial configuration is accepted as a Markov Chain member and again becomes the initial configuration for the next move. If $P^t/P^i < R$ then the trial configuration is rejected, the initial configuration is recounted as a Markov Chain member, and the next move uses the retained configuration as its starting point.

The Markov Chain is composed of many configurations, each of which is generated by a random particle move that satisfied the above criteria. The maximum allowed size of the random moves can affect how efficiently the Markov Chain is generated. If the moves are too big, there is a relatively high probability that a large percentage of configurations will be rejected because particles will be moved too close together. On the other hand, if the moves are too small, then each configuration will differ insignificantly from the last one

and it will take an excessive number of configurations to produce an average value of $f(\vec{x})$ in Equation (31). In practice, we choose the maximum allowed displacement of the random move to be $0.1(1/n_e)^{1/3}$. This choice resulted in approximately 50% of the generated configurations being included in the Markov Chain.

The Monte Carlo technique, as described above, was used to compute the ensemble average value of the cumulative distribution function $G(r)$ for a discrete set of r values. This function was evaluated for each configuration in the Markov Chain as

$$G(r) = \sum_{\substack{i=1 \\ i \neq j}}^N \theta(r - |\vec{r}_i - \vec{r}_j|) , \quad (33)$$

where θ is the step function, and the sum over i counts the pair distances $|\vec{r}_i - \vec{r}_j|$ between the j 'th particle and its $N-1$ neighbors. The prime on the sum denotes that only the $N-1$ nearest neighbor pairs were included in the evaluation of $G(r)$, and \vec{r}_j is the coordinate of the particle just moved to form the configuration under consideration. The above procedure was used by Brush et al. (1966) in the evaluation of the structure of a one-component plasma. As they pointed out, it is redundant in the long run to use pair distances in Equation (33) which do not involve the particle whose move was just accomplished.

The inclusion of only the $N-1$ nearest neighbor pairs in Equation (33) has the consequence that the cumulative distribution function will only be defined on the interval $0 \leq r \leq L/2$. One could go beyond the minimum image convention and evaluate $G(r)$ for distances greater

than $L/2$, but the periodic nature of the system and its finite size would make the accuracy of $G(r)$ at these distances questionable. To extend $G(r)$ to larger r by using bigger systems (i.e., larger N and L) requires an inordinate amount of computer time and rapidly becomes impractical.

VIII. THE PAIR POTENTIAL

The pair potential $U(r)$ representing the effective interaction between the ions in a metal can be written as (Harrison, 1966)

$$U(r) = Z^{*2}e^2/r + 2\Omega_0/(2\pi)^3 \int F(|\vec{q}|) \exp(i\vec{q} \cdot \vec{r}) d^3q, \quad (34)$$

where $F(q)$ is the energy wave number characteristic [Equation (19)] and Z^* is the effective valence of the ions [Equation (C.8)]. Z^* is found by adding up the nuclear, core electron, and orthogonalization hole charges. The first term in Equation (34) represents the direct Coulomb interaction between the ions. The second term is an indirect interaction representing the influence of the conduction electron gas. The indirect interaction is obtained from the second order contribution to the conduction electron energy E which is given in Equation (18). E contains the absolute square of the structure factor $S(q)$. This means E will include an explicit summation over pairs of atoms, and therefore, each term in the pair sum in the second-order-conduction electron energy E can be identified as an effective ion-ion potential interaction contributing to the total energy.

The $F(q)$ in Equation (34) should be consistent with the system being studied. If $U(r)$ is to be a liquid metal pair potential then $F(q)$ should be calculated for the appropriate liquid metal density. Pair potentials for Li, Na, and K were calculated using Equation (34). The results are given in Figure 11. The $F(q)$ used to obtain these $U(r)$ were calculated with the same treatment of the conduction-core

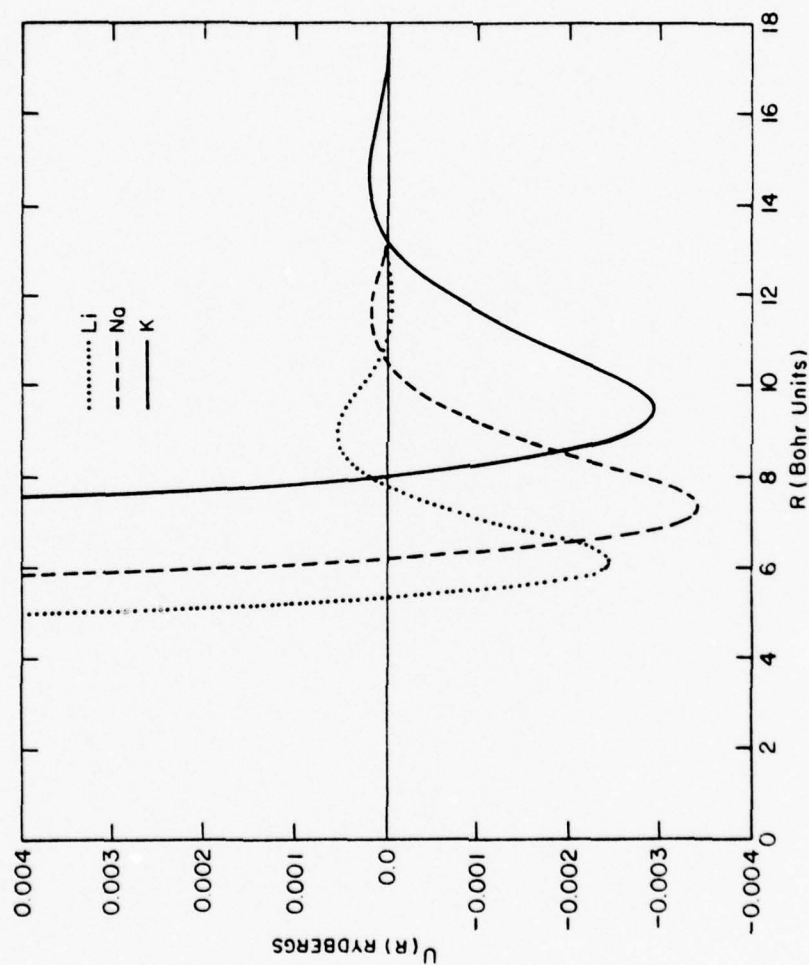


Figure 11. Pair potential curves. Liquid Li (dotted curve), Na (dashed curve), and K (solid curve) at their melting points.

exchange and dielectric screening that worked successfully in the solid metal. However, for the liquid calculation $F(q)$ used a volume per ion that was the same as the observed experimental density of the liquid.

The $U(r)$ curves in Figure 11 show several qualitative features that should be noted. First, there is a strongly repulsive core region that will keep pairs of ions from coming too close together. Also, there is a strong potential minimum which occurs at a radius that is in the vicinity of the nearest neighbor or first coordination shell distance. If the liquid were arranged in a crystalline structure, the minimum of the $U(r)$ in Figure 11 occurs at a distance that lies between the first and second nearest neighbor distances. Finally, at large r , $U(r)$ exhibits an oscillatory behavior which is a characteristic of metallic pair potentials and is due to the screening properties of the conduction electron gas (March, 1968).

IX. MONTE CARLO RESULTS FOR THE LIQUID STRUCTURE

The $U(r)$'s in Figure 11 were used to determine the cumulative distribution function $G(r)$ [i.e. equation (33)] using a Monte Carlo calculation. These functions for liquid Li, Na and K were computed at the melting temperatures and corresponding densities (see Table 3). The Monte Carlo calculations were done for systems of 125 and 216 particles initially in a cubic configuration. The first 10,000 configurations were run without averaging to let the particles evolve to more realistic configurations. Then, an additional 50,000 to 100,000 configurations were run to compute the ensemble average $G(r)$ functions for Li, Na and K. Due to the use of the minimum image convention, $G(r)$ is defined over the finite range $0 \rightarrow L/2$ (Wood and Parker, 1957).

Equation (35)

$$g(r) = 1/(4\pi r^2 n_0) \partial G(r) / \partial r \quad (35)$$

was used to calculate $g(r)$ from $G(r)$ and the results of these calculations for Li, Na and K are displayed in Figures 12, 13 and 14 respectively. These curves represent the 216 particle system. Results for the 125 particle calculations were not significantly different, indicating that many-body effects are adequately accounted for. It is to be noted that the radial distribution curves exhibit characteristic behavior, that is, at small r , $g(r)$ is zero due to core repulsion. A sharp peak occurs in $g(r)$ at intermediate r and corresponds to a coordination shell of nearest neighbors. At large r values (i.e., beyond the first peak), $g(r)$ approaches the ideal liquid limit of 1 since at these distances the liquid begins to look more and more like a continuous isotropic medium.

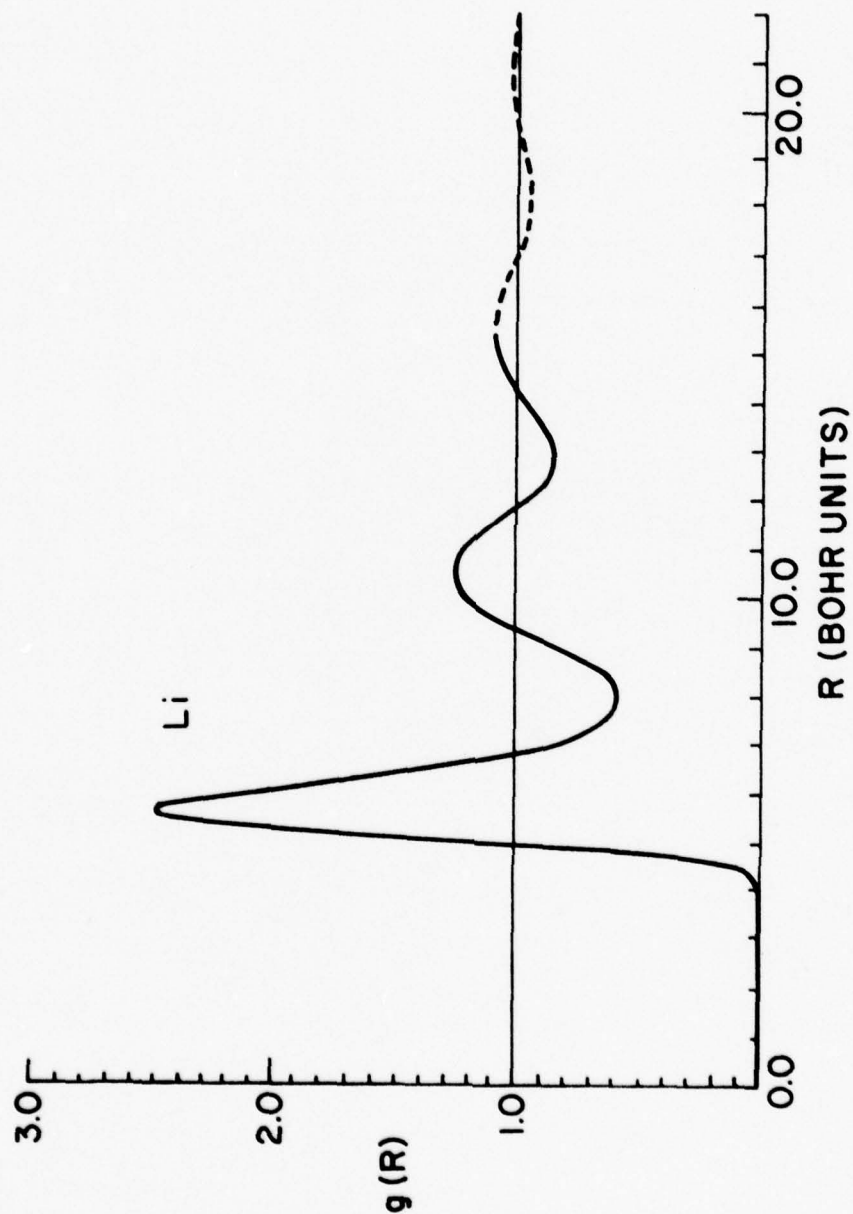


Figure 12. Radial distribution function for Li. The curve is the result of a Monte Carlo calculation using the pair potential in Figure 11.

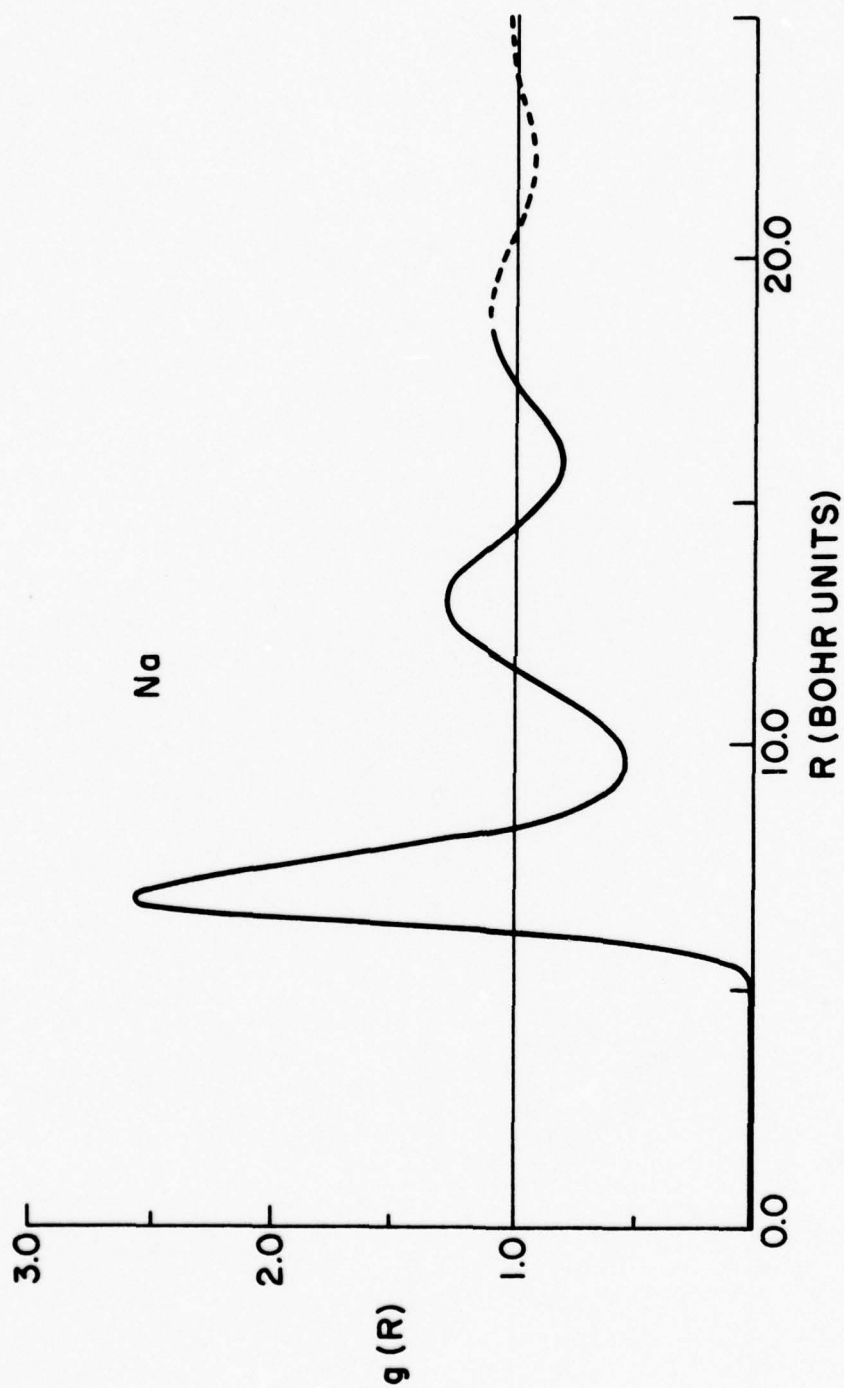


Figure 13. Monte Carlo result for the radial distribution function of Na at its melting point. The Monte Carlo calculation used the pair potential in Figure 11.

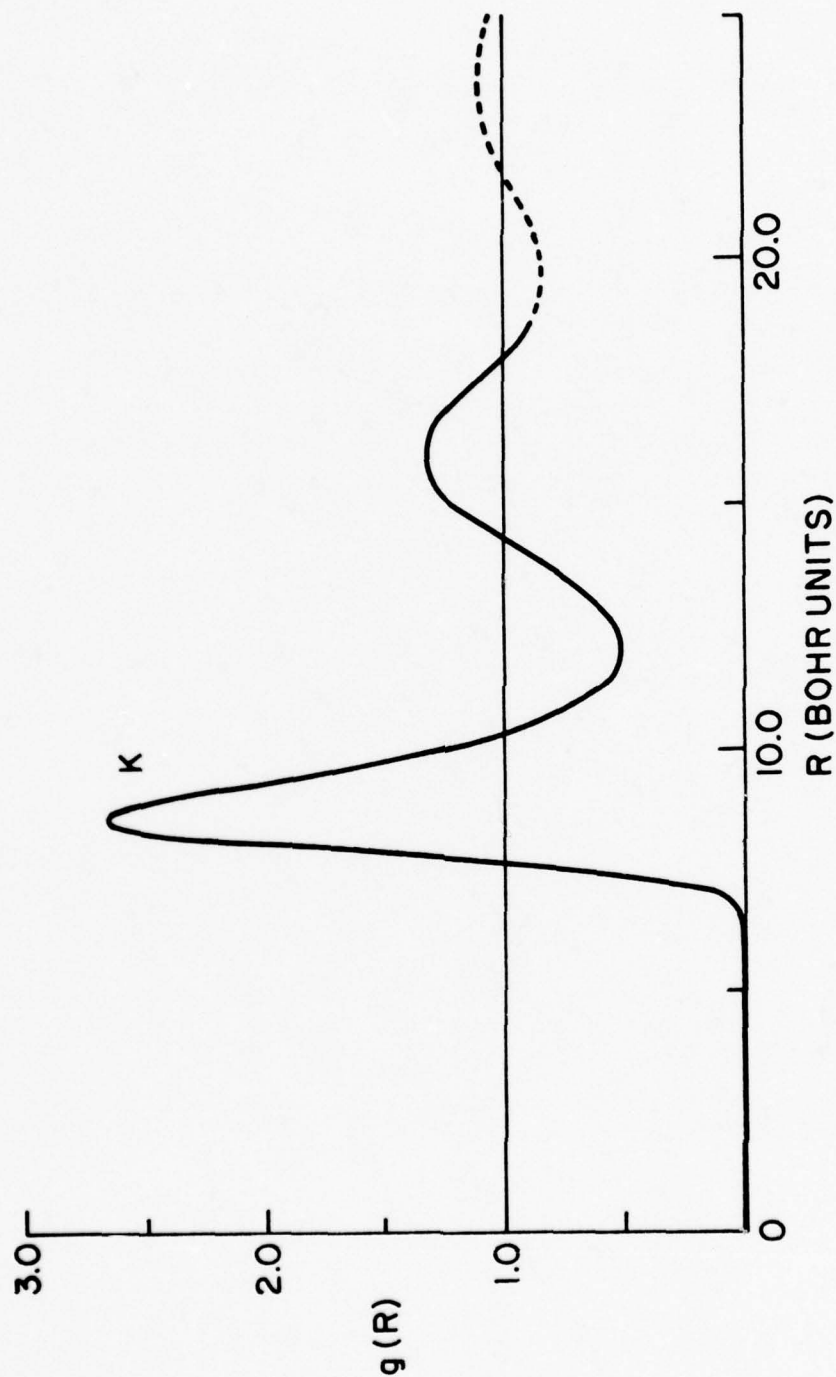


Figure 14. Monte Carlo result for the radial distribution function of K at its melting point. The Monte Carlo calculation used the pair potential in Figure 11.

Table 3. Temperature and density of Li, Na, and K at their melting point.

	$T_m (^{\circ}\text{K})$	$n_0 (\text{gm}/\text{cm}^3)$
Li	454	0.515
Na	373	0.928
K	337	0.828

The $g(r)$ curves have been extended beyond the limits of our Monte Carlo results (solid part of the curve) through the use of the Percus-Yevick theory which predicts that at large r , $g(r)$ should behave like, March (1968)

$$g(r) \approx 1 + B \cos(2K_f r + \phi) / r^3, \quad (36)$$

where B and ϕ were chosen so that there was a smooth transition between the Monte Carlo and analytic portions (dotted part) of the $g(r)$ curves.

The structure factor, $S(q)$, was calculated for the simple alkalis using Equations (26) and (27). The $S(q)$ curves in Figures 15, 16, and 17 for Li, Na and K, respectively, were obtained for $q > 2K_f$ by Fourier transforming $g(r)-1$. At low values of q [i.e., below the first peak in $S(q)$], the Fourier transform method is not accurate. Following the suggestion of Fowler (1973), $S(q)$ was calculated at low q directly from its definition in Equation (26). The explicit expression used to evaluate $S(q)$ at low q was

$$S(q) = 1/3 \sum_{\alpha=1}^3 \sum_{i=1}^N (\sin^2 q_{\alpha} x_{\alpha,i} + \cos^2 q_{\alpha} x_{\alpha,i}), \quad (37)$$

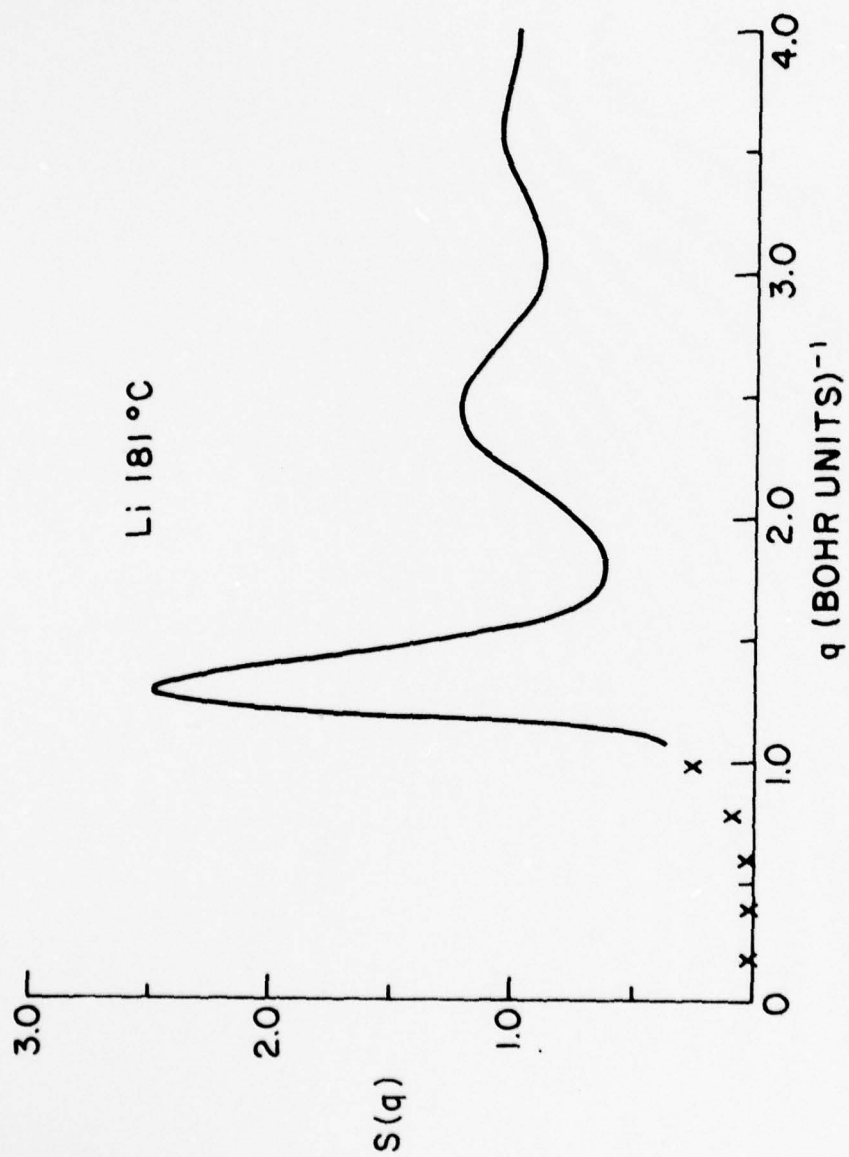


Figure 15. $S(q)$ curve for Li at its melting point.

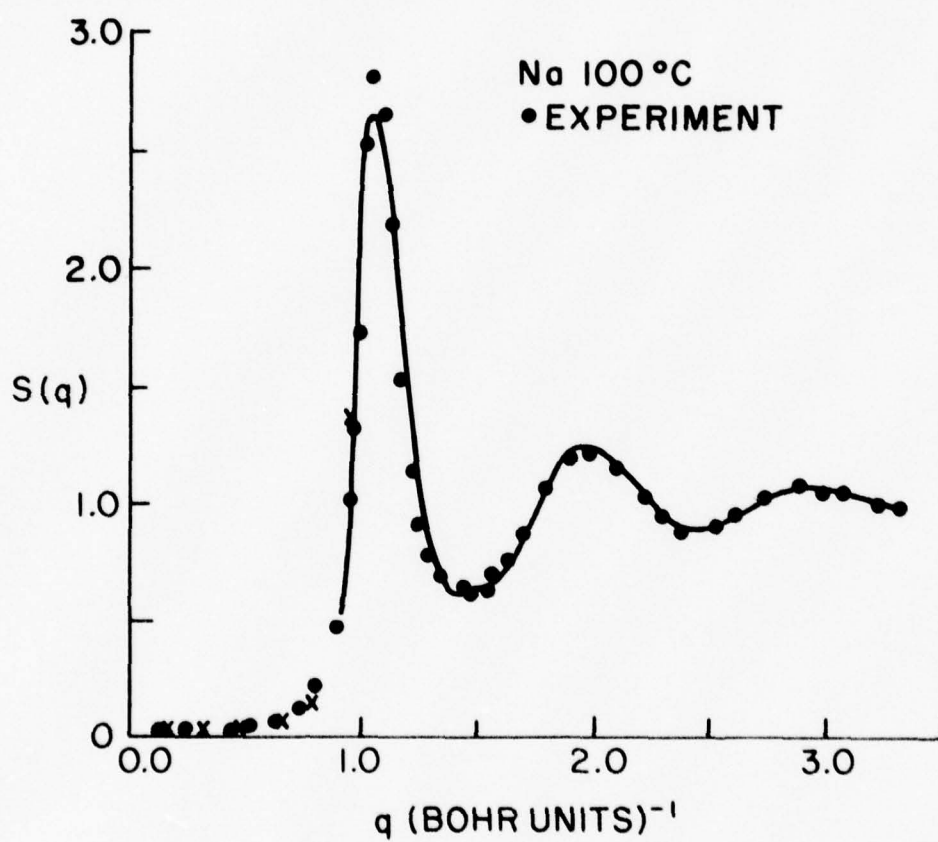


Figure 16. $S(q)$ curve for Na at its melting point. Experimental points are from Greenfield et al. (1971).

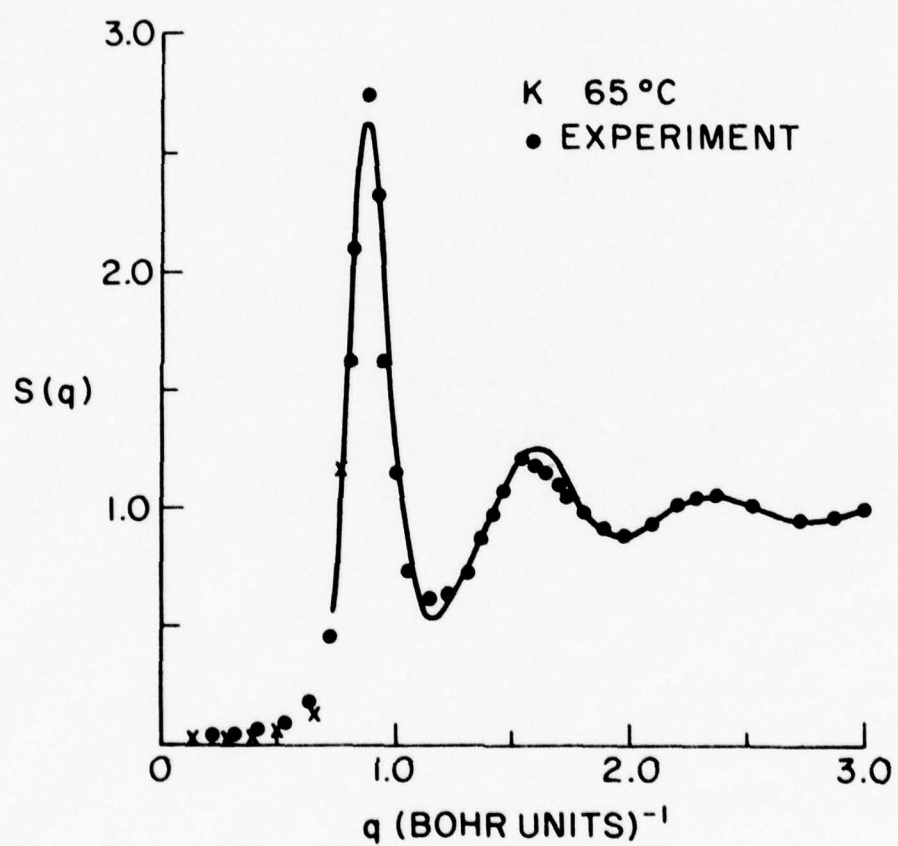


Figure 17. $S(q)$ curve for K at its melting point. Experimental points are from Greenfield et al. (1971).

where $\alpha = 1, 2, 3$ denote x, y , and z components, i is a particle label, and q was chosen as an integer multiple of $2\pi(\hat{i} + \hat{j} + \hat{k})/L$. Note that this is along a cube diagonal. As before, the bar denotes an ensemble average which was computed by using the Monte Carlo technique. The use of Equation (37) at low q to calculate $S(q)$ is much more accurate than the Fourier transform method. However, if $S(q)$ is calculated from Equation (37), there is a problem with resolution since the q values must be interger multiples of $2\pi/L$ due to the periodic boundary conditions. Calculating $S(q)$ at low q from Equation (37) is more accurate in the region $0 < q < 2K_F$, but this method will provide only a limited number of points with which we can define the $S(q)$ curve. Table 4 gives the Monte Carlo low q results for the $S(q)$ of Li, Na, and K. The experimental points in the table are interpolated from the experiments of Greenfield et al. (1971).

The $S(q)$ values for Na and K are in reasonable agreement with experimental values as can be seen from Figures 15, 16, and 17. At low q , where $S(q)$ becomes quite small, the percentage error is relatively larger but the qualitative agreement with experimental data is still excellent. $S(q)$ should approach the compressibility limit at low q

$$S(q) \approx n_0 K_B T K_t \text{ as } q \rightarrow 0, \quad (38)$$

where K_t is the isothermal compressibility, T is the temperature, and K_B is the Boltzmann constant. Greenfield et al. list the $q \rightarrow 0$ limits of $S(q)$ for Na and K as 0.0240 and 0.0247, respectively. Our calculated $S(q)$'s, though not in precise agreement with these limits, are still more

Table 4. $S(q)$ values for Li, Na, and K at low q as predicted by Monte Carlo computations. Units of q are inverse Bohr units.

Li		Na			K		
q	$S(q)$	q	$S(q)$	Exp.	q	$S(q)$	Exp.
0.196	0.0225	0.160	0.0318	0.0263	0.129	0.0212	0.0286
0.393	0.0262	0.321	0.0324	0.0321	0.258	0.0216	0.0353
0.589	0.0291	0.481	0.0415	0.0452	0.387	0.0266	0.0479
0.786	0.0703	0.642	0.0750	0.0800	0.517	0.0492	0.0800
0.983	0.246	0.802	0.152	0.196	0.646	0.133	0.218
		0.963	1.07	1.07	0.775	1.17	1.25

accurate than results employing the transform method to calculate $S(q)$ (Murphy, 1977; Murphy and Klein 1973). The analytic extension of the $g(r)$ curves heightens the first peak of the $S(q)$ curve and lowers the first minimum slightly but does not significantly affect the rest of the $S(q)$ curve. Hence the extension of $g(r)$ makes some quantitative improvements in $S(q)$ but does not make any qualitative changes.

X. LIQUID METAL ELECTRICAL RESISTIVITY

The electrical resistivity ρ_L for Li, Na and K has been calculated using Ziman's theory (Ziman, 1972)

$$\rho_L = \frac{3\pi}{4\pi e^2 v_f^2 n_0 k_f^4} \int_0^{2k_f} S(q) |w(q)|^2 q^3 dq \quad . \quad (39)$$

The equation is derived in Appendix E where the symbols are defined. The input required for this calculation is the structure factor $S(q)$ and the pseudopotential matrix element $\langle \vec{k} + \vec{q} | w | \vec{k} \rangle$ evaluated on the Fermi sphere (i.e., $|\vec{k}| = |\vec{k} + \vec{q}| = k_f$). Table 5 gives the calculated and experimental values of ρ_L for the simple alkalis. The computed values of ρ_L were obtained with our theoretically determined value of $S(q)$. For the following reason, this constitutes a more rigorous test of the pseudopotential than if the experimental $S(q)$ was used. $S(q)$ was calculated using the same pseudopotential as that used to describe the scattering potential in the calculation of the resistivity. This procedure gives us a degree of "self-consistency" vis-a-vis the ion-ion potential in the resistivity calculations. The differences between ρ_L^{th} and ρ_L^{exp} are not unreasonable when one considers the extreme sensitivity of ρ_L to both $S(q)$ and the matrix element $|\langle \vec{k} | w | \vec{k} + \vec{q} \rangle|$. Our calculations of ρ_L for various matrix elements have shown up to factor of two change in ρ_L , though the matrix elements at $q = 0$ were of the order of -0.1 rydbergs and -0.01 rydbergs at $q = q_{k_f}$. The differences were less than 1% at low q and never exceeded 0.01 rydbergs in the $2k_f$ interval for q , yet the computed resistivities

Table 5. Theoretical and experimental values for the electrical resistivity of Li, Na, and K at their melting points.

	ρ_L^{exp} ($\mu\Omega\text{-cm}$)	ρ_I^{Th} ($\mu\Omega\text{-cm}$)
Li	24.0	16.5
Na	9.7	8.0
K	13.0	8.2

differed by a factor of two. The reason for this extreme sensitivity is that the resistivity depends on the product of $S(q)$ times $|\langle \vec{k} + \vec{q} | w | \vec{k} \rangle|^2$ in the region $0 \leq q \leq k_f$. $S(q)$ is sharply peaked right around $q = 2k_f$ and will act something like a delta function. However, the matrix element undergoes a sign change in the $2k_f$ region and is rather small. Consequently, if two matrix elements differ by a small absolute amount in this region, the resistivities can be significantly different.

The matrix element in Equation (39) assumes a rather simple form because it is evaluated on the Fermi sphere [$\langle \vec{k} + \vec{q} | w | \vec{k} \rangle \rightarrow w(q)$]. It is tempting to evaluate $W(q)$ using the local approximation (ignore k dependence of the matrix element) since we are constrained to the Fermi surface. However, this local approximation significantly affects the evaluation of the screening potential $W^{\text{SC}}(q)$, which is itself local but depends on the nonlocal parts of the pseudopotential [see Equation (D.11)]. If the k dependence of the bare matrix element is ignored in evaluating the screening field, it can produce up to 40% differences in the calculation of ρ_L . Even for a simple metal like Na we find that the local approximation leads to significant errors ($\sim 20\%$) in calculations of the phonon spectra for the solid metal. Therefore the nonlocality of the pseudopotential was retained in our calculations of the resistivity.

XI. POSSIBLE IMPROVEMENTS

Consistently good results have been obtained for elastic shear constants, phonon spectra, and liquid metal structure of the simple alkali metals using a fully non local first principles pseudopotential formalism. During the course of this investigation procedures for improving the pseudopotential calculations have suggested themselves. In particular, a possible means of improving the core electron states is considered.

A first principles pseudopotential is determined to a large extent by the choice of wave functions for an ion in free space. This is a reasonable approximation for the alkalis but one must wonder if a better approximation could not be found. Sometimes the free atom wave functions are used but these do not, in principle, constitute any fundamental improvement as a representation of the core electron states in the crystal and gave greater difficulty when calculating core shifts. We would now like to suggest as an improved representation of the core states in a metal the so-called 'pseudo-atom.' A 'pseudo-atom' is an ion which is surrounded by a compensating screening charge cloud such that the ion and screening charge constitute a neutral charge system. This is approximately the case in a metal where the conduction electrons screen the ionic potentials. The well-known Herman-Skillman (1963) atomic structure program can be easily modified so that pseudo atom wave functions can be determined self consistently.

J. A. Moriarty (1974) has calculated and used simple pseudo-atom wave functions successfully in pseudopotential calculations. Moriarty's pseudo-atom was more simplistic than what we are proposing. In his calculations, the screening charge of conduction electrons was approximated by a rigid sphere of uniform charge density. The wave functions for an ion centered in this sphere were then calculated self-consistently using a modified Herman-Skillman program. One can go a step further, however, and calculate the wave functions of an ion surrounded by a spherically symmetric screening charge, where the screening potential V^{SC} can be expressed in terms of the bare ion potential and an appropriate dielectric function. It will presently be shown how this may be accomplished. First note, however, that the self-consistently calculated pseudo-atom wave functions can be applied to more than just first principles pseudopotential calculations. Improved core electron states can be used in APW and tight binding band structure calculations Calloway (1976). Also, a self consistent pseudo-atom should make an excellent representation for an impurity in a metal.

The Herman-Skillman program is designed to solve the radial part of the Schrodinger equation self consistently for the wave function $P_{n\ell}(r)$.

$$\left[\frac{-\partial^2}{\partial r^2} + \frac{\ell(\ell+1)}{r^2} + V^0(r) \right] P_{n\ell}(r) = E_{n\ell} P_{n\ell}(r) \quad (40)$$

Equation (40) is the radial Schrodinger equation, $E_{n\ell}$ is the eigenvalue for $P_{n\ell}(r)$, and the potential $V(r)$ is normally

$$v(r) = \frac{-Ze^2}{r} + 2 \int \frac{n(r') d^3 r'}{|r-r'|} + v^{ex}(r) . \quad (41)$$

The first term in Equation (41) is the nuclear coulomb potential, and the second term is the coulomb potential of the spherically averaged core electron charge density

$$n(r) = \sum_{nl}^{occup.} M_{nl} P_{nl}^2(r) / 4\pi r^2 , \quad (42)$$

where M_{nl} is the occupation number for orbital n, l . The third term is the exchange potential of the electrons which is normally approximated by a local potential. Equation (40) can be solved in an iterative manner for the $P_{nl}(r)$ and E_{nl} of a free ion or atom. The Herman-Skillman program can be converted to a pseudo-atom calculation by replacing $V^0(r)$ by $V(r)$ in Equation (40). The pseudo-atom potential $V(r)$ is

$$v(r) = v^0(r) + v^{sc}(r) , \quad (43)$$

composed of the bare potential $V^0(r)$ from Equation (41) plus a screening potential $V^{sc}(r)$. $V^{sc}(r)$ may be obtained from $V(r)$ in the following manner. First, Fourier transform $V(r)$ to obtain $V(q)$,

$$v^0(q) = \int v^0(r) e^{-iq \cdot r} d^3 r . \quad (44)$$

$v^{sc}(q)$ can be expressed in terms of $v^0(q)$ as

$$v^{sc}(q) = v^0(q) [1 - \epsilon^*(q)] / \epsilon^*(q) , \quad (45)$$

where $\epsilon^*(q)$ [see Equation (D.12)] is a static dielectric response function which, in our calculations, was chosen as the SSTL dielectric function. $v^{sc}(r)$ in equation (43) is obtained from

$$v^{sc}(r) = \frac{1}{(2\pi)^3} \int v^{sc}(q) e^{iq \cdot r} d^3q, \quad (46)$$

which is simply the inverse transform of Equation (44). The modifications to the Herman-Skillman program allow one to calculate the self consistently screened wave functions of the pseudo-atom in the linear approximation.

The pseudo-atom wave functions for Li were calculated to test the feasibility of this method. As one would expect, the first eigenvalue for the pseudo-atom was significantly less in magnitude than the ionic eigenvalue. This is, of course, due to the screening potential in the pseudo-atom calculation which causes the core charge to relax. It would be interesting to make a systematic study of the use of pseudo-atom wave functions in first principles pseudopotential calculations. (There are advantages such as the following.) A 'core shift' is calculated for the ionic eigenvalue that is the interactions between the core charge and the 10PW conduction charge density. In both Moriarty's and our pseudo-atom calculations, this interaction is taken into account in the wave function calculation, in a self consistent manner; thus, the use of the pseudo-atom leads to the elimination of the core shift in pseudopotential calculations. Our pseudo-atom calculation would not be consistent with the sphere model, but it is hoped that the inclusion of

screening in the wave function calculation is a more realistic approach. Finally, we note that one could in principle achieve a degree of self consistency between the core wave functions and the crystal potential by performing an iterative type of calculation, where, at each iteration, the core states are calculated in the field of crystalline potential (spherically symmetric part only) from the previous iteration. This would probably require a very large amount of computation but could be done.

XII. SUMMARY AND CONCLUSION

Using a first principles fully nonlocal pseudopotential, a systematic study of the simple alkali metals has been made. The phonon spectra predicted by the pseudopotential were shown to be sensitive to the exact forms of the core electron states and crystalline potential used to construct the pseudopotential. In particular, it was demonstrated that standard approximations used to describe the orthogonalization hole contribution to the conduction electron potential are, in general, inaccurate. The exact treatment of the orthogonalization hole potential was shown to produce significant changes in calculated lattice dynamical properties of the solid alkali metals Li, Na, and K.

Computer simulations of the alkalis in the liquid state were performed using pair potentials derived from our HFP fully nonlocal pseudopotential calculations. Radial distribution functions, $g(r)$, and the static structure factor, $S(q)$, were computed, using a Monte Carlo technique. Very good agreement between experimental and theoretical $S(q)$ curves was obtained. Liquid resistivity calculations were performed with a consistent treatment of the structure factor and scattering matrix elements. Specifically, Equation (39) utilized a structure factor $S(q)$ that was predicted by the same pseudopotential matrix element $W(q)$ used to describe the electron scattering in the liquid. Since the completion of this thesis research, Sun (1978) has shown that additional refinements to the present work can further improve the agreement between the calculated transport properties, resistivity, thermoelectric power, thermal conductivity, transport parameters, and experiment.

Finally, suggestions were made for improvements in calculations of the core electron states. A method for calculating self consistently screened pseudo-atom wave functions was derived. These wave functions should constitute a better representation of the core electron states in a crystal.

APPENDIX A

THEORY OF PHONONS FOR BCC STRUCTURE

In this appendix, it will be demonstrated how the phonon frequencies depend upon the energy wave number characteristic $F(|q|)$. The following discussion is limited to the case of materials with one atom per unit cell but may easily be generalized to any number of atoms per unit cell. In the harmonic approximation the potential energy of a crystal with one atom per unit cell may be written as,

$$\Phi = \Phi^0 + \frac{1}{2} \sum_{\ell, \alpha} \sum_{\ell', \beta} \Phi_{\alpha\beta}(\ell, \ell') u_{\alpha}(\ell) u_{\beta}(\ell') \quad , \quad (\text{A.1})$$

where $\Phi_{\alpha\beta}(\ell, \ell')$ is explicitly

$$\Phi_{\alpha\beta}(\ell, \ell') = \left. \frac{\partial^2 V^C}{\partial u_{\alpha}(\ell) \partial u_{\beta}(\ell')} \right|_{\substack{u_{\alpha}(\ell)=0 \\ u_{\beta}(\ell')=0}} \quad . \quad (\text{A.2})$$

The subscripts α and β denote spatial directions, $u_{\alpha}(\ell)$ and $u_{\beta}(\ell')$ are the displacements of atoms ℓ and ℓ' from equilibrium, and the second derivative of the crystalline potential V^C is evaluated at equilibrium. An equation of motion for the displacements $\vec{u}_{(\ell)}$ can be obtained by taking the gradient of Equation (A.1)

$$m \ddot{u}_{\alpha}(\ell) = - \sum_{\ell', \beta} \Phi_{\alpha\beta}(\ell, \ell') u_{\beta}(\ell') \quad . \quad (\text{A.3})$$

The phonon spectra are obtained by calculating the normal mode solutions for Equation (A.3); for a phonon of wavevector \vec{Q} and frequency

$$u_{\alpha}(\ell) = \frac{1}{\sqrt{m}} u_{\alpha}(\vec{Q}) e^{i\vec{Q} \cdot \vec{x}_{\ell}} e^{-i\omega t}, \quad (\text{A.4})$$

where \vec{x}_{ℓ} is a lattice vector. Equation (A.3) can be interpreted as representing the force on atom ℓ in the α 'th direction due to displacing the atoms ℓ' in the β direction. Substituting Equation (A.4) into Equation (A.3) yields the well known secular equation

$$\omega^2(\vec{Q}) u_{\alpha}(\vec{Q}) = \sum_{\beta} D_{\alpha\beta}(\vec{Q}) u_{\beta}(\vec{Q}). \quad (\text{A.5})$$

The dynamical matrix elements $D_{\alpha\beta}(\vec{Q})$ are defined as

$$D_{\alpha\beta}(\vec{Q}) \equiv \frac{1}{m} \sum_{\ell'} \Phi_{\alpha\beta}(\ell, \ell') e^{-i\vec{Q} \cdot (\vec{x}_{\ell} - \vec{x}_{\ell'})}. \quad (\text{A.6})$$

The phonon frequencies $\omega(\vec{Q})$ are computed by evaluating the secular determinant that is implicitly contained in Equation (A.5). The rest of this appendix will show how the dynamical matrix is evaluated.

The elements of the dynamical matrix have contributions from two different sources. These are the electrostatic energy of the ions in the crystal and the energy of the conduction-electron gas. $D_{\alpha\beta}(\vec{Q})$ is the sum of these contributions which are labelled $D_{\alpha\beta}^{\text{es}}(\vec{Q})$ and $D_{\alpha\beta}^{\text{ce}}(\vec{Q})$, respectively. The electrostatic contribution will be discussed first.

ELECTROSTATIC CONTRIBUTION TO $D_{\alpha\beta}(\vec{Q})$

The charge centered on the lattice site \vec{x}_{ℓ} , will interact with the point-ion in the ℓ' th unit cell. To compute the energy of this

interaction we must know the Coulomb potential, $v^{es}(\vec{x})$, associated with the charges centered at \vec{x}_ℓ . The potential $v^{es}(\vec{x})$ is due to the charge density

$$\rho(\vec{x}) = z^* e [\delta(\vec{x} - \vec{x}_\ell) - 1/\Omega] \quad , \quad (A.7)$$

which is composed of a positive point ion of magnitude $z^* e$ and a compensating uniform electron charge density. A gaussian charge density of half width η is added and subtracted from Equation (A.7) to make lattice sums convergent. This procedure does not alter any of the physical results. The charge density $\rho(\vec{x})$ then becomes

$$\begin{aligned} \rho(\vec{x}) &= z^* e \left\{ \left[\frac{1}{\eta^3 \pi^{3/2}} \exp [(-\vec{x} - \vec{x}_\ell)^2 / \eta^2] - 1/\Omega \right] \right. \\ &\quad \left. + \left[\delta(\vec{x} - \vec{x}_\ell) - \frac{1}{\eta^3 \pi^{3/2}} \exp [(\vec{x} - \vec{x}_\ell)^2 / \eta^2] \right] \right\} \\ &= \rho_1(\vec{x}) + \rho_2(\vec{x}) \quad , \end{aligned} \quad (A.8)$$

where $\rho_1(\vec{x})$ and $\rho_2(\vec{x})$ are the charge densities in the first and second [] brackets, respectively. The Coulomb potentials, $v_1^{es}(\vec{x})$ and $v_2^{es}(\vec{x})$, associated with $\rho_1(\vec{x})$ and $\rho_2(\vec{x})$ are evaluated as follows. The distribution $\rho_2(\vec{x})$ is spherically symmetric and Gauss' law may be used to find its electric field. Integrating over the electric field yields the potential

$$v_2^{es}(\vec{x}) = z^* e \frac{\text{erfc} |\vec{x} - \vec{x}_\ell| / \eta}{|\vec{x} - \vec{x}_\ell|} \quad . \quad (A.9)$$

Equation (A.9) excludes a constant term which disappears upon differentiation (Tosi, 1964).

It is convenient to express $\rho_1(\mathbf{x})$ as a Fourier series

$$\rho_1(\vec{\mathbf{x}}) = \sum_{\mathbf{q} \neq 0} \frac{z^* e}{\Omega} e^{-i\vec{\mathbf{q}} \cdot (\vec{\mathbf{x}}_\ell, -\vec{\mathbf{x}})} e^{-q^2 \eta^2 / 4} e^{i\vec{\mathbf{q}} \cdot \vec{\mathbf{x}}} \quad (\text{A.10})$$

where the $\mathbf{q} = 0$ term in Equation (A.10) is missing because $\rho_1(\mathbf{x})$ represents a neutral charge system. Using Poisson's equation

$$v^{es}(\mathbf{q}) \approx 4\pi \rho_1(\mathbf{q}) / q^2, \quad (\text{A.11})$$

one obtains for $v^{es}(\vec{\mathbf{x}})$,

$$v^{es}(\vec{\mathbf{x}}) = \sum_{\mathbf{q} \neq 0} \frac{4\pi z^* e}{q^2 \Omega} e^{-q^2 \eta^2 / 4} e^{-i\vec{\mathbf{q}} \cdot (\vec{\mathbf{x}}_\ell, -\vec{\mathbf{x}})} + \frac{z^* e \operatorname{erfc} |\vec{\mathbf{x}} - \vec{\mathbf{x}}_\ell| / \eta}{|\vec{\mathbf{x}} - \vec{\mathbf{x}}_\ell|}. \quad (\text{A.12})$$

The dynamical matrix elements in Equation (A.6) may be rewritten as

$$D_{\alpha\beta}^{es}(\vec{\mathbf{Q}}) = -\frac{1}{m} \sum_{\ell} \left. \frac{d v^{es}(\vec{\mathbf{x}})}{d x_\alpha d x_\beta} \right|_{\mathbf{x}=\mathbf{x}_\ell} e^{-i\vec{\mathbf{Q}} \cdot (\vec{\mathbf{x}} - \vec{\mathbf{x}}_\ell)} \quad (\text{A.13})$$

In Equation (A.13), the derivatives of $v^{es}(\vec{\mathbf{x}})$ are taken with respect to $\vec{\mathbf{x}}$ and not the displacements \mathbf{u} as in Equation (A.6). The function $v^{es}(\vec{\mathbf{x}})$ differs from $v^{es}(\mathbf{x})$ by a factor $z^* e$. Hence, by substituting $z^* e$ times Equation (A.12) into Equation (A.13) one obtains

$$D_{\alpha\beta}^{es}(\vec{Q}) = \frac{1}{m} \sum_{\ell'} \left\{ \sum_{\vec{q} \neq 0} \frac{4\pi z^{*2} e^2}{q^2 \Omega} q_{\alpha} q_{\beta} e^{-q^2 \eta^2 / 4} e^{-i\vec{q} \cdot (\vec{x}_{\ell'} - \vec{x}_{\ell})} \right. \\ \left. - z^{*2} e^2 \frac{\partial^2}{\partial x_{\alpha} \partial x_{\beta}} \frac{\text{erfc}|\vec{x} - \vec{x}_{\ell'}|/\eta|}{|\vec{x} - \vec{x}_{\ell'}|} \right\}_{\vec{x} = \vec{x}_{\ell}} e^{-i\vec{Q} \cdot (\vec{x}_{\ell} - \vec{x}_{\ell'})} \quad (\text{A.14})$$

It is apparent that the above expression for $D_{\alpha\beta}^{es}$ is a function of $\vec{x}_{\ell} - \vec{x}_{\ell'}$, which must also be a lattice vector. Therefore, in Equation (A.14), it is possible to replace $\vec{x}_{\ell} - \vec{x}_{\ell'}$ by \vec{x}_{ℓ} and $\sum_{\ell'}$ by \sum_{ℓ} . Note that when $\ell = \ell'$, the second term in Equation (A.14) is singular. This difficulty may be circumvented by making use of the condition

$$\Phi_{\alpha\beta}(\ell, \ell') = - \sum_{\ell' \neq \ell} \Phi_{\alpha\beta}(\ell, \ell') \quad (\text{A.15})$$

which results from the fact that the system is invariant under a uniform translation. Utilizing Equation (A.15) and the above considerations results in Equation (A.16) for $D_{\alpha\beta}^{es}$

$$D_{\alpha\beta}^{es} = \frac{z^{*2} e^2}{m} \sum_{\ell=0} \left\{ - \sum_{\vec{q} \neq 0} \frac{4\pi}{q^2 \Omega} q_{\alpha} q_{\beta} e^{-q^2 \eta^2 / 4 - i\vec{q} \cdot \vec{x}_{\ell}} + \frac{\partial^2}{\partial x_{\alpha} \partial x_{\beta}} \frac{\text{erfc}|\vec{x}|/\eta|}{|\vec{x}|} \right\}_{\vec{x} = \vec{x}_{\ell}} \\ \times \left(1 - e^{-i\vec{Q} \cdot \vec{x}_{\ell}} \right) \quad (\text{A.16})$$

Equation (A.16) may be simplified by using the lattice sum rule

$$\sum_{\ell=0}^N e^{-i\vec{q} \cdot \vec{x}_{\ell}} = N \delta_{\vec{q}, \vec{G}} \quad (\text{A.17})$$

Making use of Equation (A.17) to eliminate the ℓ sum in the first term of Equation (A.16), and explicitly differentiating the erfc, one obtains

$$\begin{aligned}
 D_{\alpha\beta}^{\text{es}}(\vec{Q}) = & \frac{4\pi z^{*2} e^2}{m\Omega_0} \sum_{\vec{G}}' \left[\frac{(\vec{G}+\vec{Q})_{\alpha} (\vec{G}+\vec{Q})_{\beta}}{|\vec{G}+\vec{Q}|} e^{-|\vec{G}+\vec{Q}|^2 \eta^2/4} - \frac{G_{\alpha} G_{\beta}}{G^2} e^{-G^2 \eta^2/4} \right] \\
 & + \frac{z^{*2} e^2}{m} \sum_{\ell \neq 0} \left\{ \frac{x_{\ell, \alpha} x_{\ell, \beta}}{x_{\ell}^2} \left[\frac{3 \text{erfc}|\vec{x}_{\ell}|/\eta}{x_{\ell}^3} + \frac{6e^{-x_{\ell}^2/\eta}}{\eta \sqrt{\pi} x_{\ell}^2} + \frac{4e^{-x_{\ell}^2/\eta^2}}{\eta^3 \sqrt{\pi}} \right] \right. \\
 & \left. - \delta_{\alpha\beta} \left[\frac{2e^{-x_{\ell}^2/\eta}}{\eta x_{\ell}^2 \sqrt{\pi}} + \frac{\text{erfc}|\vec{x}_{\ell}|/\eta}{x_{\ell}^3} \right] \right\} \left(1 - e^{i\vec{Q} \cdot \vec{x}_{\ell}} \right). \quad (\text{A.18})
 \end{aligned}$$

The prime on the G sum indicates that, when $G = 0$, the term with $1/G^2$ is eliminated.

THE CONDUCTION ELECTRON CONTRIBUTION TO $D_{\alpha\beta}$

The conduction electron contribution to $D_{\alpha\beta}$ will now be considered. The energy of the conduction electron gas depends on the crystal structure through Equation (18) which we duplicate here for convenience

$$E = \sum_{\vec{q}} S(\vec{q}) S^*(\vec{q}) F(\vec{q}) \quad (\text{A.19})$$

The structure factor $S_{(\vec{q})}$ is a function of the lattice coordinates. For a crystal with one atom per unit cell, it may be written as

$$S(\vec{q}) = \frac{1}{N} \sum_{\ell} e^{-i\vec{q} \cdot (\vec{x}_{\ell} + \vec{u}_{\ell})} \quad (\text{A.20})$$

where N is the number of unit cells, \vec{x}_ℓ is the position of atom ℓ , and \vec{u}_ℓ is its displacement from equilibrium. It is convenient to expand $S(q)$ in terms of the displacement, \vec{u}_ℓ

$$S(q) = \frac{1}{N} \sum_{\ell} e^{i\vec{q} \cdot \vec{x}_\ell} \left[1 - i\vec{q} \cdot \vec{u}_\ell + \frac{(-i\vec{q} \cdot \vec{u}_\ell)^2}{2!} + \dots \right] \quad (A.21)$$

For a pure normal mode of wave vector \vec{Q} , the lattice displacement \vec{u}_ℓ may be written as

$$\vec{u}_\ell = \frac{1}{\sqrt{m}} \left[\vec{U}(\vec{Q}) e^{i\vec{Q} \cdot \vec{x}_\ell} + \vec{U}^*(\vec{Q}) e^{-i\vec{Q} \cdot \vec{x}_\ell} \right] \quad (A.22)$$

In Equation (A.22) the normal mode displacement has been expressed in a form that ensures that it is real. Substituting u_ℓ into Equation (A.21) and using Equation (A.17), $S(q)$ becomes

$$\begin{aligned} S(q) = & \delta_{q,G} - \frac{i\vec{q}}{\sqrt{m}} \cdot \left[\vec{U}(\vec{Q}) \delta_{\vec{q}-\vec{Q},\vec{G}} e^{-i\omega t} + \vec{U}^*(\vec{Q}) \delta_{\vec{q}+\vec{Q},\vec{G}} e^{i\omega t} \right] \\ & + \frac{-1}{2m} \left[[\vec{q} \cdot \vec{U}(\vec{Q})]^2 \delta_{\vec{q}+2\vec{Q},\vec{G}} e^{-2i\omega t} + 2\vec{q} \cdot \vec{U}(\vec{Q}) \vec{q} \cdot \vec{U}^*(\vec{Q}) \delta_{\vec{q},\vec{G}} \right. \\ & \left. + [\vec{q} \cdot \vec{U}^*(\vec{Q})]^2 \delta_{\vec{q}-2\vec{Q},\vec{G}} e^{2i\omega t} \right] + \dots \quad (A.23) \end{aligned}$$

The product $S^*(q)$ in Equation (A.19) will be nonzero only when the Kronecker deltas in the product have similar arguments. Retaining only terms up to second order in the displacements, one obtains the following for the conduction electron energy change due to the normal mode displacements

$$\begin{aligned}
\Delta E = \frac{1}{m} \sum_{\vec{G}} & \left[\sum_{\alpha, \beta} (\vec{G} + \vec{Q})_{\alpha} (\vec{G} + \vec{Q})_{\beta} U_{\alpha}^{*}(\vec{Q}) U_{\beta}(\vec{Q}) F(|\vec{G} + \vec{Q}|) \right. \\
& + \sum_{\alpha, \beta} (\vec{G} - \vec{Q})_{\alpha} (\vec{G} - \vec{Q})_{\beta} U_{\alpha}(\vec{Q}) U_{\beta}^{*}(\vec{Q}) F(|\vec{G} - \vec{Q}|) \left. \right] \\
& - 2 \sum_{\alpha, \beta} G_{\alpha} G_{\beta} U_{\alpha}(\vec{Q}) U_{\beta}^{*}(\vec{Q}) F(|\vec{G}|) . \quad (A.24)
\end{aligned}$$

In Equation (A.24), α and β denote the cartesian components x, y, z , and the factors $\vec{G} + \vec{Q}$ and $\vec{G} - \vec{Q}$ are equivalent because of the sum over G -vectors. Equation (A.24) represents the energy difference of the conduction electrons between the equilibrium lattice ($\vec{u}_l = 0$) and the distorted lattice. An equivalent expression in terms of the dynamical matrix can be obtained by combining Equations (A.1), (A.6), and (A.22) (include a sum over Q) to find the second order energy change per ion caused by a lattice displacement. This is given by

$$\Phi - \Phi^0 = \frac{1}{2} \sum_{\alpha\beta} D_{\alpha\beta}(\vec{Q}) U_{\alpha}^{*}(\vec{Q}) U_{\beta}(\vec{Q}) + D_{\alpha\beta}^{*}(\vec{Q}) U_{\alpha}(\vec{Q}) U_{\beta}^{*}(\vec{Q}) . \quad (A.25)$$

Comparing Equations (A.24) and (A.25) results in the conduction electron contribution to the dynamical matrix. This is given by

$$D_{\alpha\beta}^{ce}(\vec{Q}) = \frac{2}{m} \sum_{\vec{G}} \left[(\vec{G} + \vec{Q})_{\alpha} (\vec{G} + \vec{Q})_{\beta} F(|\vec{G} + \vec{Q}|) - G_{\alpha} G_{\beta} F(|\vec{G}|) \right] , \quad (A.26)$$

where the $\vec{G} = 0$ term involving $F(|\vec{G}|)$ is omitted from the sum. Hence, with Equations (A.26) and (A.18), the phonon frequencies $\omega(\vec{Q})$ can be determined by evaluating the secular determinant in Equation (A.5).

APPENDIX B

ELASTIC CONSTANTS FOR BODY CENTERED CUBIC MATERIALS

In general the elastic energy density W is related to the elastic constants C_{ij} and the strains e_i through the following relationship

$$W = W_0 + \frac{1}{2} \sum_{i,j=1}^6 C_{ij} e_i e_j \quad (B.1)$$

This equation is only valid for small deformations and is based on Hooke's Law or, equivalently, the harmonic approximation. W_0 represents the energy per ion of the undeformed (i.e., equilibrium) crystal. The strains e_i are defined as follows

$$\begin{aligned} e_1 &= \frac{\partial u}{\partial x}, & e_2 &= \frac{\partial v}{\partial y}, & e_3 &= \frac{\partial w}{\partial z}, & e_4 &= \frac{\partial w}{\partial y} + \frac{\partial v}{\partial z}, \\ e_5 &= \frac{\partial u}{\partial z} + \frac{\partial w}{\partial x} & \text{and } e_6 &= \frac{\partial u}{\partial y} + \frac{\partial v}{\partial x}, \end{aligned} \quad (B.2)$$

where u , v , w are the x , y , and z components of the displacement in a crystal caused by a deformation. e_1 , e_2 , e_3 are related to distortions of the x , y , and z axis, and e_4 , e_5 , e_6 describe angular deformations of the angle between the axis defining the yz , xz , and xy planes, respectively.

It can be shown that, at most, there are 21 independent elastic constants. Body centered cubic (bcc) materials have only three independent elastic constants. Thus, for a bcc crystal, it suffices to calculate three constants designated by C_{11} , C_{12} , and C_{44} in order to specify the elastic properties of the material since the other elastic constants are either zero or equal to one of these. In the rest of this section, two specific volume conserving strains will be considered

that can be related to C_{11} , C_{12} , and C_{44} with the aid of Equation (B.1).

Consider the vectors describing a primitive unit cell for a bcc crystal before and after a deformation. If $\vec{a}_1, \vec{a}_2, \vec{a}_3$ are the primitive vectors before the strain, and $\vec{a}'_1, \vec{a}'_2, \vec{a}'_3$ are the vectors after the strain, then they are related by the strain matrix \bar{e}

$$\begin{aligned}\vec{a}'_1 - \vec{a}_1 &= \bar{e} \vec{a}_1 = (u_1, v_1, w_1) \\ \vec{a}'_2 - \vec{a}_2 &= \bar{e} \vec{a}_2 = (u_2, v_2, w_2) \\ \vec{a}'_3 - \vec{a}_3 &= \bar{e} \vec{a}_3 = (u_3, v_3, w_3) \quad ,\end{aligned}\tag{B.3}$$

where the strain matrix \bar{e} is

$$\bar{e} = \begin{bmatrix} e_1 & e_6/2 & e_5/2 \\ e_6/2 & e_2 & e_4/2 \\ e_5/2 & e_4/2 & e_3 \end{bmatrix} \quad .\tag{B.4}$$

Hence, if the vectors \vec{a}_1 and \vec{a}'_1 are known, then the strains e_i can be obtained through Equations (3) and (4) as there are nine equations and only six unknowns.

The bcc primitive vectors in the unstrained state are

$$\vec{a}_1 = \frac{a}{2} (1, 1, -1), \quad \vec{a}_2 = \frac{a}{2} (-1, 1, 1) \text{ and } \vec{a}_3 = \frac{a}{2} (1, -1, 1), \tag{B.5}$$

where a is the lattice constant. Now, if the z axis is stretched and the x and y axis compressed so that the primitive cell volume is

conserved (see Figure 18) (i.e., $\vec{a}_1 \cdot \vec{a}_2 \times \vec{a}_3 = \vec{a}'_1 \cdot \vec{a}'_2 \times \vec{a}'_3$), then the vectors may be expressed as

$$\begin{aligned}\vec{a}'_1 &= \frac{a}{2} (\epsilon_1^{\ell/2}, \epsilon_1^{\ell/2}, -\epsilon_1^{-\ell}) \\ \vec{a}'_2 &= \frac{a}{2} (-\epsilon_1^{\ell/2}, \epsilon_1^{\ell/2}, \epsilon_1^{-\ell}) \\ \vec{a}'_3 &= \frac{a}{2} (\epsilon_1^{\ell/2}, -\epsilon_1^{\ell/2}, \epsilon_1^{-\ell})\end{aligned}\quad . \quad (B.6)$$

ϵ_1 is the strain parameter which is equal to 1 at equilibrium and ℓ is arbitrary and can be chosen for convenience. Substituting Equations (B.4), (B.5), and (B.6) into Equation (B.3) results in a system of coupled equations for the e_i . Solving this set of simultaneous equations, one obtains the strain matrix elements e_i in terms of the parameter ϵ_1 . Now that the e_i are known as function of ϵ_1 , it is relatively easy to show, using Equation (B.1), that the second derivative of W evaluated at equilibrium ($\epsilon_1 = 1$) is

$$\left. \frac{\partial^2 W}{\partial \epsilon_1^2} \right|_0 = \frac{3\ell^2}{2} (C_{11} - C_{12}) \quad . \quad (B.7)$$

Having defined a deformation ϵ_1 that is related to the elastic constants C_{11} and C_{12} , we now consider a deformation ϵ_2 which can be related to the C_{44} elastic constant. The constant C_{44} is related to a shear that changes the angle between the z and x axis. An alternative way of viewing this shear is that vectors along $(1,1,1)$ expand while vectors that are perpendicular contract or vice-versa (see Figure 18). Hence, the deformation ϵ_2 takes the vectors

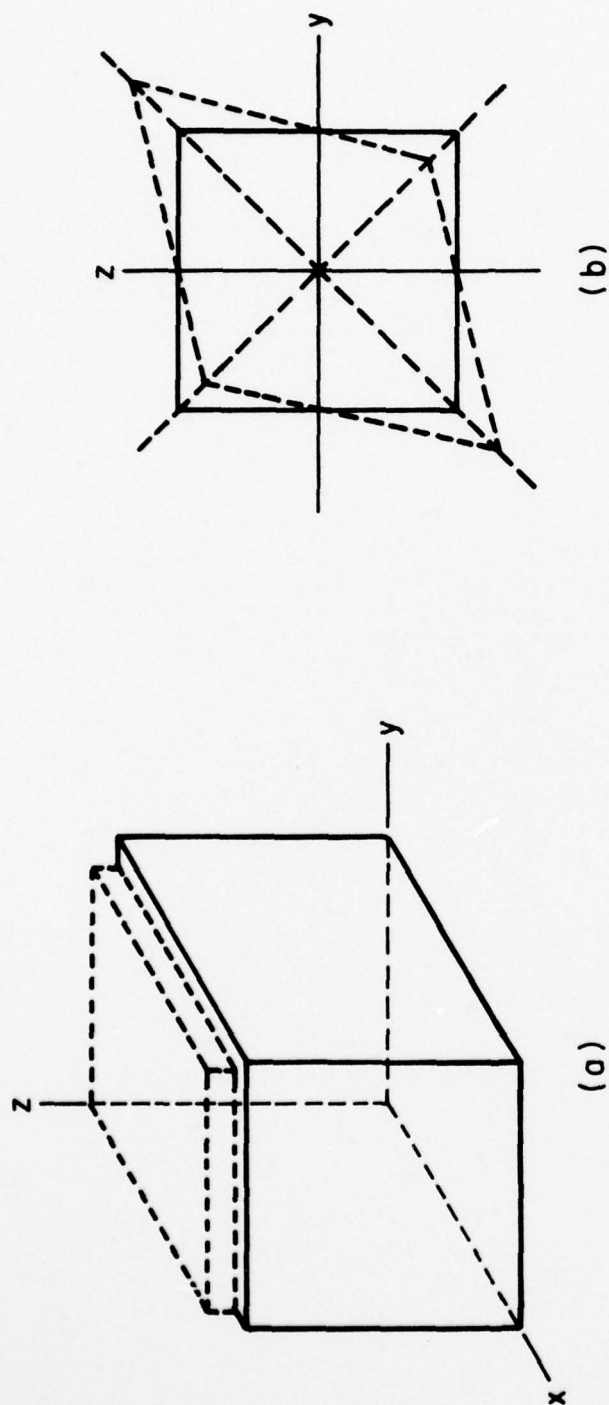


Figure 18. Volume conserving elastic shears from a bcc system.

- (a) $C_{11}-C_{12}$ strain shortens the x and y axis and lengthens the z axis.
- (b) C_{44} strain bends the angle between the z and y axis which is equivalent to an expansion and contraction along a set of axes that are rotated by 45° with respect to the z - y axis.

$$\vec{s}_1 = (1,1,-1), \quad \vec{s}_2 = (1,-1,0), \quad \vec{s}_3 = (1,0,-1) \quad (\text{B.8})$$

and transforms them to

$$\vec{s}'_1 = A(1,1,-1), \quad \vec{s}'_2 = B(1,-1,0), \quad \vec{s}'_3 = B(1,0,-1) \quad . \quad (\text{B.9})$$

Taking Equations (B.3), (B.4), (B.8), and (B.9) it may be shown that

$$e_1 = e_2 = e_3 = \frac{A + 2B - 3}{3}$$

$$\text{and} \quad e_4 = e_5 = e_6 = \frac{2}{3} (A-B) \quad . \quad (\text{B.10})$$

It may further be shown that $B = A^{-1/2}$ in order to ensure volume conservation of the primitive unit cell. Finally, if A is replaced by ϵ_2^{ℓ} , then

$$\left. \frac{\partial^2 W}{\partial \epsilon_2^2} \right|_0 = 3\ell^2 C_{44} \quad , \quad (\text{B.11})$$

where subscript 0 indicates the derivative is evaluated at equilibrium.

We have now defined deformations ϵ_1 and ϵ_2 that are related to $C_{11} - C_{12}$ and C_{44} through the second derivative of the elastic energy density. To evaluate these constants, it is necessary to derive an expression for W , which is the energy per ion. This energy is composed of two parts that will give nonzero contributions to the derivatives in Equations (B.7) and (B.11). W consists of W^{ce} , the conduction electron energy, and W^{es} , the electrostatic energy per ion. W^{es} represents the average electrostatic energy per ion in a crystal, where the crystal is visualized as a regular array of point positive

charges immersed in a compensating uniform electron sea. w^{es} will be evaluated with the aid of a technique developed by Ewald for producing convergent lattice sums. The other contribution, w^{ce} , is the structurally dependent part of the conduction-electron energy. Actually, w^{ce} has been encountered previously as the quantity E in Equations (18) and (A.19). It is the second order contribution to the conduction electron energy. The zero and first order contributions to the electronic energy, being structurally independent, do not contribute to the derivatives in Equations (B.7) and (B.11). The sum of w^{es} and w^{ce} give the energy of a primitive unit cell in the crystal. The square of the structure factor, $S(q)$, in Equation (18) is responsible for the explicit dependence of w^{ce} upon the crystal structure. For a perfect lattice, the absolute square of $S(q)$ is

$$\begin{aligned} |S(\vec{q})|^2 &= \frac{N}{N^2} \sum_{\vec{\ell}} e^{-i\vec{q} \cdot \vec{x}_{\ell}} \\ &= \delta_{\vec{q}, \vec{G}} \end{aligned} \quad (B.12)$$

In Equation (B.13), \vec{x}_{ℓ} represents a lattice vector, \vec{G} a reciprocal lattice vector and N is the number of unit cells in the crystal. Hence Equation (18) becomes, with the aid of Equation (B.12)

$$w^{ce} = \sum_{\vec{G}}' F(\vec{G}) \quad (B.13)$$

The electrostatic energy w^{es} is a rather complicated expression so we shall give some of the details of its derivation. The charge density of the crystal can be written as

AD-A058 828

PENNSYLVANIA STATE UNIV UNIVERSITY PARK APPLIED RESE--ETC F/G 7/2
FIRST PRINCIPLES PSEUDOPOTENTIAL CALCULATIONS OF ELECTRONIC AND--ETC(U)
JUL 78 R S DAY N00017-73-C-1418
ARL-PSU-TM-78-194 NL

UNCLASSIFIED

2 of 2

AD
A058 828



$$\rho(\vec{x}) = z^*e \left\{ \sum_{\ell} \delta(\vec{x} - \vec{x}_{\ell}) - \frac{1}{\Omega_0} \right\} , \quad (\text{B.14})$$

and its Fourier components are, therefore

$$\begin{aligned} \rho(\vec{q}) &= \frac{1}{\Omega} \int \rho(\vec{x}) e^{-i\vec{q} \cdot \vec{x}} d^3x \\ &= \frac{z^*e}{\Omega} \left\{ \sum_{\ell} e^{-i\vec{q} \cdot \vec{x}_{\ell}} - \frac{\Omega}{\Omega_0} \delta_{\vec{q},0} \right\} . \end{aligned} \quad (\text{B.15})$$

The Coulomb potential associated with $\rho(\vec{x})$ is

$$\begin{aligned} \phi(\vec{x}) &= \sum_{\vec{q}} \frac{4\pi}{q^2} \rho(\vec{q}) e^{i\vec{q} \cdot \vec{x}} \\ &= \frac{4\pi z^*e}{\Omega_0} \sum'_{\vec{G}} \frac{e^{i\vec{G} \cdot \vec{x}}}{G^2} , \end{aligned} \quad (\text{B.16})$$

where Ω_0 is the primitive cell volume, z^*e the charge of an ion in the crystal, and the prime on the \vec{G} sum denotes that the $\vec{G} = 0$ term is omitted. However, one should note that Equation (B.16) does not represent a converging sum. We must resort to a method due to Ewald to obtain a convergent sum equivalent to Equation (B.16). One may easily verify that

$$\phi(\vec{x}) = \frac{z^*4\pi e}{\Omega_0} \sum'_{\vec{G}} \int_0^{\infty} e^{-G^2\xi + i\vec{G} \cdot \vec{x}} d\xi . \quad (\text{B.17})$$

Equation (B.17) is identical to Equation (B.16). Factoring the integral into different domains of integration

$$\phi(\vec{x}) = \frac{4\pi z^*e}{\Omega_0} \left\{ \int_0^{\eta} e^{-G^2\xi + i\vec{G} \cdot \vec{x}} d\xi + \int_{\eta}^{\infty} e^{-G^2\xi + i\vec{G} \cdot \vec{x}} d\xi \right\} , \quad (\text{B.18})$$

and making use of the theta transformation (Born and Huang, 1954) yields

$$\phi(\vec{x}) = \sum_{\ell} z^* e \int_0^{\eta} \frac{1}{2\sqrt{\pi\xi^3}} e^{-(\vec{x}_{\ell}-\vec{x})^2/4\xi} d\xi - \frac{4\pi z^* e}{\Omega_0} \int_0^{\eta} d\xi + \frac{4\pi z^* e}{\Omega_0} \sum_{\ell} \frac{e^{-G^2\eta + i\vec{G}\cdot\vec{x}}}{G^2} . \quad (B.19)$$

Equation (B.19) represents the Coulomb potential at \vec{x} due to all charge in the crystal. Subtracting the potential due to the point charge at \vec{x}'_{ℓ} from Equation (B.19), letting $\eta \rightarrow \frac{1}{2\sqrt{\eta}}$, and setting $\vec{x} = \vec{x}'_{\ell}$, we obtain

$$\phi'(\vec{x}'_{\ell}) = \sum_{\ell} \frac{z^* e \operatorname{erfc} \eta |\vec{x}'_{\ell}|}{|\vec{x}'_{\ell}|} + \frac{4\pi z^* e}{\Omega_0} \sum_{\ell} \frac{e^{-G^2/4\eta^2}}{G^2} - \frac{4\pi z^* e}{\Omega_0 \eta^2} - \frac{2\eta z^* e}{\sqrt{\pi}} , \quad (B.20)$$

which is the potential at $\vec{x}'_{\ell} = 0$ due to all charges in the crystal except the point ion at $\vec{x}'_{\ell} = 0$.

In the above we determined the potential ϕ' which was the potential due to all but one charge in the crystal. The single charge is omitted in deriving Equation (B.20) since it is not correct to have a charge interact with itself when the interaction energy of the system is computed. ϕ' may be related to W^{es} as follows

$$W^{\text{es}} = \frac{1}{2} z^* e \phi' = \frac{z^* e^2}{2} \left\{ \sum_{\ell} \frac{\operatorname{erfc} \eta |\vec{x}'_{\ell}|}{|\vec{x}'_{\ell}|} + \sum_{\ell} \frac{4\pi}{\Omega_0 G^2} e^{-G^2/4\eta^2} - \frac{\pi}{\Omega_0 \eta^2} - \frac{2\eta}{\sqrt{\pi}} \right\} . \quad (B.21)$$

Expressions (B.13) for W^{ce} , and (B.21) for W^{es} can be put into either Equation (B.7) or (B.11) to compute the elastic constants

$$\begin{aligned}
 \frac{\partial^2 W}{\partial \epsilon_i^2} &= \frac{\partial^2 W^{ce}}{\partial \epsilon_i^2} + \frac{\partial^2 W^{es}}{\partial \epsilon_i^2} \quad i = 1, 2 \\
 &= \sum_G \left(\frac{\partial^2 F(G)}{\partial G^2} G'^2 + \frac{\partial F(G)}{\partial G} G'' \right) \\
 &\quad + \frac{e^2 z^{*2}}{2} \sum_{\ell} \left\{ \frac{2}{\sqrt{\pi}} \left[\frac{-\eta x_{\ell}''}{x_{\ell}} + x_{\ell}'^2 \left(\frac{2\eta}{x_{\ell}^2} + 2\eta^3 \right) \right] e^{-\eta^2 x_{\ell}^2} \right. \\
 &\quad \left. + \operatorname{erfc} \eta |x_{\ell}| \left[\frac{2x_{\ell}'^2}{x_{\ell}^3} - \frac{x_{\ell}''}{x_{\ell}^2} \right] \right. \\
 &\quad \left. + \sum_G \frac{4\pi z^{*2} e^{-G^2/4\eta^2}}{\Omega_0} \left[G'^2 \left(\frac{6}{G^4} + \frac{3}{2\eta^2 G^2} + \frac{1}{4\eta^4} \right) - G'' \left(\frac{2}{G^3} + \frac{1}{2\eta^2 G} \right) \right] \right\}.
 \end{aligned} \tag{B.22}$$

G' , G'' , x_{ℓ}' , x_{ℓ}'' are, respectively, the first and second derivatives of the reciprocal and real lattice vectors with respect to ϵ_1 or ϵ_2 and the other quantities have been previously defined. With Equation (B.22), we have all the information needed to calculate the elastic constants C_{11} , C_{12} and C_{44} for a bcc crystal. The quantities G' , G'' , x_{ℓ}' , x_{ℓ}'' can be evaluated easily since $x_{\ell}(\epsilon_i)$ and $G(\epsilon_i)$ are known because the strain matrix $\bar{\epsilon}$ has previously been evaluated for the deformations ϵ_1 and ϵ_2 .

APPENDIX C

THE ORTHOGONALIZATION HOLE

The orthogonalization hole (OH) density is one component of the conduction electron charge density. In this appendix an exact expression for $n^{\text{OH}}(\vec{r})$ is derived and compared with the standard approximations of Harrison (1966). The core shift due to the interaction of $n^{\text{OH}}(\vec{r})$ with the core-electron density, V^{opw} is computed below with both the approximate and exact forms of $n^{\text{OH}}(\vec{r})$.

The conduction-electron charge density, $n^{\text{cond}}(\vec{r})$, is obtained by taking the absolute square of $\psi_{\vec{k}}^{\text{C}}(\vec{r})$ and summing over all occupied k states.

$$n^{\text{cond}}(\vec{r}) = \sum_{\vec{k}}^{k_f} \phi_{\vec{k}}^*(\vec{r}) (1 - P^*) (1 - P) \phi_{\vec{k}}(\vec{r}) \quad . \quad (\text{C.1})$$

Equation (7) was used to obtain expression (C.1) for the conduction-electron density. Substituting equation (6) into (C.1) and keeping only zero or first order terms, $n^{\text{cond}}(\vec{r})$ becomes,

$$n^{\text{cond}}(\vec{r}) = \sum_{\vec{k}}^{k_f} \left\{ \frac{1}{\Omega} - \frac{e^{-i\vec{k} \cdot \vec{r}}}{\sqrt{\Omega}} P|\vec{k}\rangle - \frac{e^{i\vec{k} \cdot \vec{r}}}{\sqrt{\Omega}} \langle \vec{k}|P^* + \langle \vec{k}|P^* \cdot P|\vec{k}\rangle \right. \\ \left. + \frac{1}{\Omega} \sum_{\vec{q} \neq 0} \left[a_{\vec{q}}^*(\vec{k}) e^{+i\vec{q} \cdot \vec{r}} + a_{\vec{q}}(\vec{k}) e^{-i\vec{q} \cdot \vec{r}} \right] \right\} \quad . \quad (\text{C.2})$$

Plane wave states not being operated upon by the projection operator have been shown explicitly.

The fact that $a_{q=0}(\vec{k}) = 1$ has also been used in the derivation of Equation (C.2), the 2nd, 3rd, and 4th terms of Equation (C.2) comprise $n^{\text{OH}}(\vec{r})$ while the last term constitutes the screening charge density $n^{\text{SC}}(\vec{r})$. The OH density is essentially determined once the core-electron wave functions have been specified, whereas $n^{\text{SC}}(\vec{r})$ represents the self-consistent response of the electron gas to the perturbing potential $W(\vec{r})$.

It is convenient to make the following substitutions in Equation (C.2). The core eigenstates in the projection operator $P = \sum_{n\ell} |n\ell\rangle\langle n\ell|$ are explicitly

$$|n\ell\rangle = P_{n\ell}(r) Y_{\ell}^m(\theta, \phi)/r \quad . \quad (\text{C.3})$$

Also, the plane waves may be expanded as

$$e^{i\vec{k}\cdot\vec{r}} = \sum_{\ell} [4\pi(2\ell+1)]^{1/2} j_{\ell}(kr) i^{\ell} Y_{\ell}^0(\theta, \phi) \quad , \quad (\text{C.4})$$

where $P_{n\ell}(r)$ is the radial part of the core wave function, j_{ℓ} is a spherical Bessel function, and Y_{ℓ}^m is a spherical harmonic. With Equations (C.3) and (C.4) in Equation (C.2), $n^{\text{OH}}(\vec{r})$ can be expressed as

$$n^{\text{OH}}(\vec{r}) = \frac{-4\Omega_0}{(2\pi)^3} \int_0^{k_f} \sum_{n\ell} \frac{(2\ell+1) \langle k | n\ell \rangle P_{n\ell}(r)}{r} \left[\frac{\sqrt{4\pi}}{\Omega_0} j_{\ell}(kr) - \sum_{n'} \frac{P_{n'\ell}(r) \langle k | n'\ell \rangle}{2r} \right] k^2 dk \quad . \quad (\text{C.5})$$

The quantity $\langle k | n\ell \rangle$ is known as an orthogonality coefficient and is given by

$$\langle k | n\ell \rangle = \frac{4\pi}{\Omega_0} \int j_\ell(kr) P_{n\ell}(r) r dr . \quad (C.6)$$

The expressions (C.2) for $n^{\text{cond}}(\vec{r})$ and (C.5) for $n^{\text{OH}}(\vec{r})$ are not correct as they stand because the conduction wave functions are not normalized. If $n^{\text{cond}}(\vec{r})$ is integrated over all space, one finds for the total charge of a primitive unit cell

$$\int n^{\text{cond}}(\vec{r}) d^3r = 1 - \langle \vec{k} | P | \vec{k} \rangle . \quad (C.7)$$

Hence, $n^{\text{OH}}(\vec{r})$ and $n^{\text{cond}}(\vec{r})$ should be divided by the factor $1 - \langle \vec{k} | P | \vec{k} \rangle$ to ensure the correct normalization for the conduction charge density. When the normalization factor in Equation (C.7) is included in Equations (C.2) and (C.5), one finds that there are effectively Z^* electrons in $n^{\text{sc}}(\vec{r})$ and $Z_V - Z^*$ electrons in $n^{\text{OH}}(\vec{r})$, where

$$Z^* = \frac{2\Omega_0}{(2\pi)^3} \int \frac{d^3k}{1 - \langle \vec{k} | P | \vec{k} \rangle} . \quad (C.8)$$

Z^* is the effective valence of the metal, and Z_V is the classical valence (e.g., $Z_V = 1$ for Li, Na, K). The effective valence Z^* will always be slightly greater than Z_V since $\langle \vec{k} | P | \vec{k} \rangle$ is a positive definite quantity.

The charge density $n^{\text{OH}}(\vec{r})$ (properly normalized) will give rise to two effects. Firstly, its Coulomb potential $V^{\text{OH}}(\vec{r})$ will contribute to the crystalline potential $V^{\text{C}}(\vec{r})$, and secondly, $n^{\text{OH}}(\vec{r})$ will interact with the core charge $n^{\text{core}}(\vec{r})$ to shift the core eigenvalues by an amount called

V^{opw} . The potential $V^{\text{OH}}(r)$ was evaluated by performing a standard Coulomb integral over the spherically symmetric charge density $n^{\text{OH}}(\vec{r})$. Then the energy shift of the n, ℓ 'th core state is given by

$$V_{n\ell}^{\text{opw}} = e^2 \int P_{n\ell}^2(r) V^{\text{OH}}(r) dr \quad . \quad (\text{C.9})$$

The matrix element of $V^{\text{OH}}(r)$ is also needed in the evaluation of the pseudopotential, and with the aid of Poisson's equation can be shown to be

$$\langle k + q | V^{\text{OH}}(r) | k \rangle = \frac{4\pi e^2}{q^2 \Omega_0} n^{\text{OH}}(q) \quad , \quad (\text{C.10})$$

where $n^{\text{OH}}(q)$ is the Fourier transform of $n^{\text{OH}}(\vec{r})$.

Equation (C.5) constitutes an exact expression for $n^{\text{OH}}(\vec{r})$ when the normalization factor (C.7) is included. All calculations in this thesis were done with the exact form of $n^{\text{OH}}(\vec{r})$. Harrison (1966) originally proposed using approximate treatments of $n^{\text{OH}}(\vec{r})$ and V^{opw} because of the difficulty in evaluating the exact $n^{\text{OH}}(\vec{r})$. However as will be shown these approximations are rather severe and can lead to significant errors. Harrison used the following approximation for the matrix element of $V^{\text{OH}}(r)$

$$\langle \vec{k} + \vec{q} | V^{\text{OH}}(r) | \vec{k} \rangle^{\text{H}} = \frac{4\pi e^2}{q^2 \Omega_0} \frac{n^{\text{core}}(q)}{n^{\text{core}}(q=0)} (Z_V - Z^*) \quad . \quad (\text{C.11})$$

Equation (C.11) is based on the assumption that the OH is distributed in the same manner as the core-electron charge density. The OH

core shift on the other hand was approximated by

$$V^{\text{OPW-H}} = \frac{-\Omega_0}{\pi^2} \sum_{n\ell} 2(2\ell+1) \left(\frac{\int P^2(r) dr}{r} \right) \left(\int \langle k | n\ell \rangle^2 k^2 dk \right) \quad (C.12)$$

In Equation (C.12), the OH is approximated as a point charge of magnitude $Z_V = Z^*$ located at the nucleus. Clearly, this is a rather crude approximation.

It is instructive to compare the exact treatment of the OH [i.e., Equations (A.5), (C.9), (C.10)] with the approximate treatments [i.e., Equations (C.11) and (C.12)]. Table 6 shows calculated exact and approximate values of V^{OPW} for Li, Na, and K. The approximate V^{OPW} is roughly a factor of 2 to 3 too large and is not a function of n and ℓ as it should be. Cutler et al. (1975) showed for zinc that the differences in these two treatments of V^{OPW} can lead to significant changes in calculated lattice dynamical properties such as the phonon spectra. Li, Na, and K also are affected by the differences in V^{OPW} .

The approximate and exact treatments of $n^{\text{OH}}(\vec{r})$ yield quite different results. Figure 19 shows the exact $n^{\text{OH}}(\vec{r})$ for Li, Na, and K that were used to calculate $V^{\text{OH}}(\vec{r})$. Notice that $n^{\text{OH}}(\vec{r})$ changes sign in certain regions of r . When the approximate $V^{\text{OH}}(\vec{r})$ is calculated, $n^{\text{OH}}(\vec{r})$ is assumed to have the same spatial distribution as the core electrons. Hence, the approximate $n^{\text{OH}}(\vec{r})$ will not exhibit any changes in sign and is therefore not even in qualitative agreement with the exact treatment.

Table 6. Exact versus approximate V^{opw} for Li, Na, and K.

	Exact V^{opw}	Approximate V^{opw}	Energies in Rydbergs
Li	-0.0743 ^{1s}	-0.2659	
Na	-0.0594 ^{1s} -0.0868 ^{2s} -0.0851 ^{2p}	-0.1870	
K	-0.0988 ^{1s} -0.1117 ^{2s} -0.1103 ^{2p} -0.1235 ^{3s} -0.1232 ^{3p}	-0.2029	

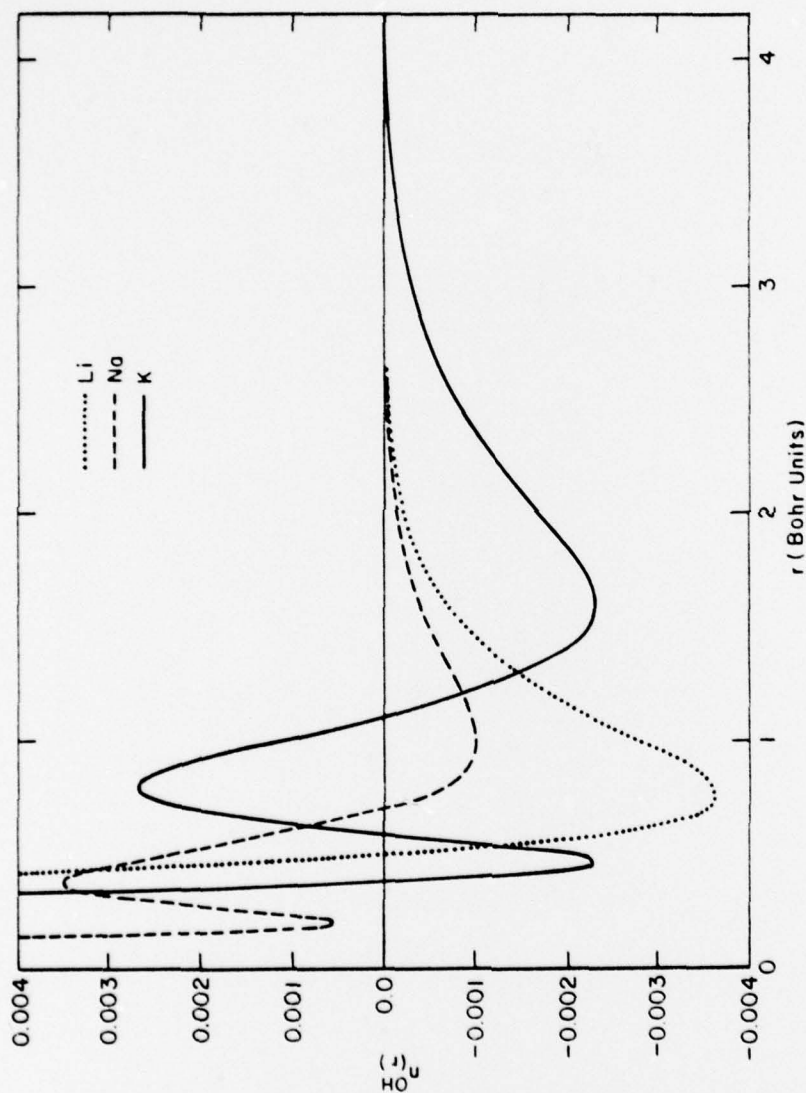


Figure 19. Exact $n^{OH}_{\vec{r}}(r)$ for Li, Na, and K. Multiply scales for Li, Na, and K by 2, 4, and 1, respectively.

APPENDIX D

SCREENING OF THE PSEUDOPOTENTIAL

This appendix presents a brief derivation of the screening contribution to the pseudopotential. The conduction-electron charge density [i.e., Appendix C, Equation (C.2)] consists of the orthogonalization hole density which was discussed in detail in Appendix C and the screening charge density which is explicitly

$$n^{sc}(\vec{r}) = \sum_{\vec{k}}^f \frac{1}{\Omega} \left[1 + \sum_{\vec{q} \neq 0} \left(a_{\vec{q}}^*(\vec{k}) e^{-i\vec{q} \cdot \vec{r}} + a_{\vec{q}}(\vec{k}) e^{i\vec{q} \cdot \vec{r}} \right) \right] \quad (D.1)$$

The coefficients $a_{\vec{q}}(\vec{k})$ were previously used to expand $\psi_{\vec{k}}^{cond}(\vec{r})$ and $\phi_{\vec{k}}(\vec{r})$ in terms of opw's and plane waves, respectively. First order perturbation theory applied to Equation (4), the pseudopotential equation, yields $a_{\vec{q}}(\vec{k})$ as

$$a_{\vec{q}}(\vec{k}) = \frac{\langle \vec{k} + \vec{q} | W | \vec{k} \rangle}{\frac{\hbar^2}{2m} (k^2 - |\vec{k} + \vec{q}|^2)} \quad (D.2)$$

Equation (D.1) can be rewritten

$$n^{sc}(\vec{r}) = \frac{2}{(2\pi)^3} \int d^3k \left\{ 1 + \sum_{\vec{q} \neq 0} \left[a_{-\vec{q}}^*(\vec{k}) + a_{\vec{q}}(\vec{k}) \right] e^{i\vec{q} \cdot \vec{r}} \right\} \quad (D.3)$$

where the sum over k has been converted to an integration in the standard manner. Now, if one notes that $a_{\vec{q}}(\vec{k}) = a_{-\vec{q}}^*(-\vec{k})$ and that

$a_{-\vec{q}}^*(\vec{k})$ may be replaced by $a_{-\vec{q}}^*(-\vec{k})$ due to the symmetric k integration,
 $n^{sc}(\vec{r})$ may be conveniently expressed as

$$n^{sc}(\vec{r}) = \frac{2}{(2\pi)^3} \int d^3k \left\{ 1 + 2 \sum_{q \neq 0} \frac{\langle \vec{k} + \vec{q} | W | \vec{k} \rangle}{\frac{\hbar^2}{2m}(k^2 - |\vec{k} + \vec{q}|^2)} e^{i\vec{q} \cdot \vec{r}} \right\} . \quad (D.4)$$

Interchanging the orders of the integration and summation and expressing $n^{sc}(\vec{r})$ as a Fourier transform leads to

$$n^{sc}(\vec{r}) = \sum_{\vec{q}} n^{sc}(\vec{q}) e^{i\vec{q} \cdot \vec{r}} , \quad (D.5)$$

where

$$n^{sc}(\vec{q}) = \begin{cases} \frac{4}{(2\pi)^3} \int d^3k \frac{\langle \vec{k} + \vec{q} | W | \vec{k} \rangle}{\frac{\hbar^2}{2m}(k^2 - |\vec{k} + \vec{q}|^2)} & q \neq 0 \\ \frac{2}{(2\pi)^3} \int d^3k = Z \sqrt{\Omega_0} & q = 0 \end{cases} . \quad (D.6)$$

When the correct normalization of the conduction wavefunction is used (see Appendix C), the $q = 0$ Fourier coefficient will have the value Z^*/Ω_0 . The Fourier components of $n^{sc}(\vec{r})$ for nonzero q represent the perturbative response of the conduction-electron gas to the perturbing potential $W(r)$. We shall now describe how the response of the conduction gas to the perturbing potential $W(r)$ can be made self-consistent. We will also show how exchange and correlation effects between conduction electrons can be incorporated into the description of screening.

In Equation (D.6), it is possible to make the screening self-consistent by using Poisson's equation and by separating $W(r)$ into a bare unscreened potential $W^b(r)$ and the Coulomb potential of the screening electrons $W^{SC}(r)$. The Fourier transforms of $n^{SC}(r)$ and $W^{SC}(r)$ are related by Poisson's equation.

$$W^{SC}(q) = \frac{4\pi e^2}{q^2} n^{SC}(q) [1 - G(q)] \quad (D.7)$$

The Coulomb interaction has been modified by the exchange and correlation interaction between the electrons in the conduction gas and this is explicitly taken into account by the extra factor of $1 - G(q)$ in Equation (D.7) (Singwi et al., 1968). Using Equation (D.7) in Equation (D.6) and separating W into $W^b + W^{SC}$, one obtains

$$\begin{aligned} \frac{W^{SC}(q)q^2[1-G(q)]}{4\pi e^2} &= \frac{4}{(2\pi)^3} W^{SC}(q) \int \frac{d^3k}{\frac{\hbar^2}{2m}(k^2 - |\vec{k} + \vec{q}|^2)} \\ &+ \frac{4}{(2\pi)^3} \int \frac{\langle \vec{k} + \vec{q} | W^b | \vec{k} \rangle d^3k}{\frac{\hbar^2}{2m}(k^2 - |\vec{k} + \vec{q}|^2)} \quad (D.8) \end{aligned}$$

In Equation (D.8), $W^{SC}(q)$ is factored out of the integrand because it is independent of \vec{k} . Taking note of the fact that (Bardeen, 1937)

$$\int \frac{d^3k}{\frac{\hbar^2}{2m}(k^2 - |\vec{k} + \vec{q}|^2)} = \frac{\pi^2 q^2}{2e^2} [1 - \epsilon(q)] \quad (D.9)$$

where

$$\epsilon(q) = 1 + \frac{2me^2}{n\hbar^2 q^2} \left(k_f + \frac{k_f^2 - q^2/4}{q} \ln \left| \frac{2k_f + q}{2k_f - q} \right| \right), \quad (D.10)$$

one may show that

$$W^{sc}(q) = \frac{2e^2}{q^2 \pi^2} \frac{[1 - G(q)]}{\epsilon^*(q)} \left\{ \frac{\langle \vec{k} + \vec{q} | W^b | \vec{k} \rangle}{\frac{\hbar^2}{2m}(k^2 - |\vec{k} + \vec{q}|^2)} d^3k \right\}. \quad (D.11)$$

The function $\epsilon^*(q)$ is the static dielectric response function for an interacting electron gas. It is related to the free electron or so-called Hartree static dielectric function $\epsilon(q)$ by

$$\epsilon^*(q) = 1 + [1 - G(q)][\epsilon(q) - 1]. \quad (D.12)$$

Equation (D.11) for the screening contribution to the pseudo-potential indicates that one may express the screening potential in terms of the bare perturbing potential and a dielectric screening function $\epsilon^*(q)$. The matrix element of the bare or unscreened part of the pseudopotential $\langle \vec{k} + \vec{q} | W^b | \vec{k} \rangle$ is given in Equation (14). In local pseudopotential calculations, the matrix element of W^b is factored out of the integrand in Equation (D.11) and a very simple relation is thus obtained between $W^b(q)$ and $W^{sc}(q)$.

$$W^{sc}(q) = \frac{[1 - \epsilon^*(q)]}{\epsilon^*(q)} W^b(q). \quad (D.13)$$

Although this is a widely used approximation, it was not used in any calculations in this thesis because the bare potential matrix elements are not independent of \vec{k} as implied by this approximation. The matrix element of $V^C(r)$ in Equation (14) is independent of \vec{k} and could be factored out of the integrand in Equation (D.11), but the remaining terms in Equation (14) are nonlocally dependent on both the magnitude and direction of \vec{k} . The local approximation significantly alters the screening field and consequently affects the predictions of lattice dynamical properties. Therefore, the full nonlocal form of the pseudopotential was used in all our calculations.

APPENDIX E

DERIVATION OF THE LIQUID METAL RESISTIVITY EXPRESSION

Ziman's formula (Ziman, 1961) for the electrical resistivity ρ of liquid metal was given in Equation (39) where k_f , v_f , n_0 , $w(q)$, $S(q)$, e , and q are the Fermi wavenumber, Fermi velocity, average number density, pseudopotential form factor, liquid structure factor, electronic charge, and momentum transferred in a scattering process, respectively. We will now briefly discuss Equation (39) and indicate what approximations are inherent in this formula.

The current density J for a system of charged particles in a volume Ω subject to an electric field \vec{F} along the z axis can be expressed in terms of the distribution function $f(k)$.

$$J_Z = \frac{1}{\Omega} \sum_k e v_z f(k) \quad . \quad (E.1)$$

Converting the sum over occupied k states to an integral in the standard manner yields,

$$J_Z = \frac{2e}{(2\pi)^3} \int v_z f(k) d^3k \quad . \quad (E.2)$$

If the distribution function is a linear function of \vec{F} , then the scalar conductivity σ and, subsequently, the resistivity ρ can be determined from the relation $\vec{J} = \sigma \vec{F}$. To find \vec{J} or σ , we must first calculate $f(k)$. For a system that is in a steady state, Liouville's equation states that,

$$df(k)/dt = 0 \quad . \quad (E.3)$$

It is convenient to reexpress the total time derivative as a sum of partial time derivatives. Ignoring diffusion and assuming zero magnetic field, the distribution function $f(k)$ will change with time because of the field \vec{F} and scattering processes. Hence, Equation (E.3) is equivalent to

$$\frac{\partial f(k)}{\partial t_{\text{field}}} + \frac{\partial f(k)}{\partial t_{\text{scat}}} = 0, \quad (\text{E.4})$$

where

$$\frac{\partial f(k)}{\partial t_{\text{field}}} = - \frac{\partial f(k)}{\partial k} \frac{k_z}{k} \frac{eF}{\hbar} \quad (\text{E.5})$$

and

$$\frac{\partial f(k)}{\partial t_{\text{scat}}} = \int f(k') [1-f(k)] P_{k'k} d^3k' - \int f(k) [1-f(k')] P_{kk'} d^3k' \quad (\text{E.6})$$

The function $P_{kk'}$ is the probability for a transition from the state k to the state k' . Combining Equations (E.4), (E.5), (E.6) and writing $f(k)$ as the sum of an equilibrium contribution, $f^0(k)$, and a contribution $g(k)$ due to the electric field results in

$$\frac{\partial f^0(k)}{\partial k} \frac{k_z}{k} \frac{eF}{\hbar} = \int [g(k') - g(k)] P_{kk'} d^3k' \quad (\text{E.7})$$

Equation (E.7) was obtained by keeping only terms linear in \vec{F} [note that $g(k)$ is proportional to F so that we are limited to small signals] and assuming that $P_{kk'} = P_{k'k}$.

The electric field changes the k_z component of an electron's \mathbf{k} vector by an amount eFt/\hbar in time t . However, the scattering processes tend to offset the momentum gain of the electron caused by the electric field. If the electric field were turned off, we would expect \vec{J} to decay exponentially with a characteristic relaxation time τ that is determined by the scattering mechanism. Similarly, the Fermi distribution would change in time due to the electric field if the scattering processes did not stop the electrons momentum from increasing indefinitely. It is easily seen that the perturbation part of the distribution function, $g(\mathbf{k})$, can be expressed as

$$g(\mathbf{k}) = \frac{\partial f^0(\mathbf{k})}{\partial k} \frac{eF}{\hbar} \frac{k_z}{k} \tau, \quad (\text{E.8})$$

where τ is a characteristic relaxation time of the system. To obtain a solution for $g(\mathbf{k})$, we assume the Born approximation for $P_{\mathbf{k}\mathbf{k}'}$,

$$P_{\mathbf{k}\mathbf{k}'} = \frac{2\Omega}{(2\pi)^3} |W_{\mathbf{k}\mathbf{k}'}|^2 \frac{\pi}{\hbar} \delta(E_{\mathbf{k}} - E_{\mathbf{k}'}) \quad (\text{E.9})$$

where $W_{\mathbf{k}\mathbf{k}'}$ is the matrix element of the scattering potential between the states \mathbf{k} and \mathbf{k}' . Using Equations (E.8) and (E.9) in Equation (E.7) yields the following result for the relaxation time τ

$$\frac{1}{\tau} = \int \left(1 - \frac{k'_z}{k_z} \right) |W_{\mathbf{k}\mathbf{k}'}|^2 \frac{m\Omega k'}{2\pi\hbar^3} d \cos \theta \quad (\text{E.10})$$

where θ is the angle between $\vec{\mathbf{k}}$ and $\vec{\mathbf{k}'}$. The use of the Born approximation means that $\vec{\mathbf{k}}$ and $\vec{\mathbf{k}'}$ both lie on the same energy sphere (i.e., $|\vec{\mathbf{k}}| = |\vec{\mathbf{k}}'|$).

The expression for τ gives us complete knowledge of $f(k)$ and it is now a trivial matter to formally calculate the current density J

$$J_z = \frac{2e}{(2\pi)^3} \int \frac{v_z k_z}{k_f} \frac{eF}{\hbar} \frac{\partial f^0(k)}{\partial k} \tau d^3k \quad . \quad (E.11)$$

Assuming that $\partial f^0/\partial k$ is a sharply peaked function of the Fermi surface

$$J_z = \frac{4e^2 k_f^3 \tau}{m(2\pi)^2} F \quad . \quad (E.12)$$

It is obvious from Equation (E.12) that the resistivity ρ for the metal is

$$\rho = \frac{3(2\pi)^2 m}{4e^2 k_f^3 \tau} \quad , \quad (E.13)$$

which, after some algebra, coordinate changes, and factorizing of the pseudopotential matrix element, in the expression for $1/\tau$ reduces to Equation (39).

Some general comments may be in order at this point. In the derivation for ρ , it was assumed that there was a sharp Fermi surface so that $\partial f^0/\partial \epsilon$ was a delta function at this surface. However, one can estimate that, if the temperature blurring of f^0 was taken into account, the correction to ρ would be roughly four orders of magnitude smaller than the results obtained with the sharp Fermi surface assumption.

BIBLIOGRAPHY

- I. Abarenkov and V. Heine, *Phil. Mag.* 12, 529 (1965).
- A. O. E. Animalu, *Phil. Mag.* 11, 379 (1965).
- N. W. Ashcroft, *Phys. Lett.* 23, 48 (1966).
- J. Bardeen, *Phys. Rev.* 52, 688 (1937).
- J. A. Bearden and A. F. Burr, *Rev. Mod. Phys.* 39, 125 (1967).
- M. Born and K. Huang, *Dynamical Theory of Crystal Lattices* (Oxford University Press, London, 1954).
- M. Born and H. S. Green, *Proc. Roy. Soc. A* 188, 10 (1946).
- S. G. Brush, H. Sahlin, and E. Teller, *J. Chem. Phys.* 45, 2802 (1966).
- J. Calloway, *Quantum Theory of the Solid State* (Academic Press, Inc., New York, 1976).
- CRC Handbook of Chemistry and Physics*, 53rd ed., edited by R. C. Weast (Chemical Rubber Co., Cleveland, Ohio, 1972).
- M. H. Cohen and V. Heine, *Phys. Rev.* 122, 1821 (1961).
- R. A. Cowley, A. D. Woods, and G. Dolling, *Phys. Rev.* 150, 487 (1966).
- C. A. Croston, *Liquid State Physics - A Statistical Mechanical Introduction* (Cambridge University Press, 1974).
- P. H. Cutler, R. S. Day, and W. F. King, III, *J. Phys. F: Metal Phys.* 6, L1 (1976).
- L. Dagens, *J. Phys. C: Solid State Phys.* 5, 2333 (1972).
- L. Dagens, M. Rosolt, and R. Taylor, *Phys. Rev.* B11, 2726 (1975).
- R. S. Day, F. Sun, P. H. Cutler, and W. F. King, III, *J. Phys. F: Metal Phys.* 6, L137 (1976).
- M. E. Diederich and J. Trivisonno, *J. Phys. Chem. Solids* 27, 637 (1966).
- T. E. Faber, *Introduction to the Theory of Liquid Metals* (Cambridge University Press, 1972).
- R. H. Fowler, *J. Chem. Phys.* 59, 3435 (1973) and private communications.
- D. J. W. Geldart and R. Taylor, *Can. J. Phys.* 48, 167 (1970).

- A. J. Greenfield, J. Wellendorf, and N. Wiser, Phys. Rev. A4, 1607 (1971).
- J. Hafner, J. Phys. F: Metal Phys. 5, 1439 (1974).
- J. Hafner and P. Schmuck, Phys. Rev. B9, 4138 (1974).
- F. S. Ham, Phys. Rev. 128, 1524 (1962).
- W. A. Harrison, Phys. Rev. 129, 2503 (1963).
- W. A. Harrison, Phys. Rev. 129, 2512 (1963).
- W. A. Harrison, Phys. Rev. 136, 1107 (1964).
- W. A. Harrison, Phys. Rev. 181, 1036 (1969).
- W. A. Harrison, Pseudopotentials in the Theory of Metals (W. A. Benjamin, Reading, Mass., 1966).
- V. Heine and D. Weire, Solid State Phys. 24, 249 (1970).
- F. Herman and J. Skillman, Atomic Structure Calculations (Prentice-Hall, Inc., Englewood Cliffs, N. J., 1963).
- C. Herring, Phys. Rev. 57, 1169 (1940).
- M. Jain and S. C. Jain, Phys. Rev. B7, 4338 (1973).
- W. F. King, III and P. H. Cutler, Phys. Rev. B8, 1303 (1973).
- W. Kohn and L. J. Sham, Phys. Rev. 140, A1133 (1965).
- P. J. Lin and J. C. Phillips, Advan. Phys. 14, 257 (1965).
- I. Lindgren, Int. J. Quant. Chem. 5, 411 (1971).
- I. Lindgren and K. Schwarz, Phys. Rev. A5, 542 (1972).
- N. H. March, Liquid Metals (Pergamon Press, Oxford, 1966).
- N. H. March, "Effective Ion-Ion Interaction in Liquid Metals" in Physics of Simple Liquids, edited by H. N. V. Temperley, J. S. Rowlinson and G. S. Rushbrooke (North-Holland Publishing Co., Amsterdam, 1968).
- W. R. Marquardt and J. Trivisonno, J. Phys. Chem. Solids 26, 273 (1965).
- N. A. Metropolis, A. W. Rosenbluth, M. N. Rosenbluth, A. H. Teller, and E. Teller, J. Chem. Phys. 21, 1087 (1953).
- J. A. Moriaty, Phys. Rev. B1, 1363 (1970).

- J. A. Moriarty, Phys. Rev. B10, 3075 (1974).
- R. D. Murphy, Phys. Rev. A15, 1188 (1977).
- R. D. Murphy and M. L. Klein, Phys. Rev. A8, 2640 (1973).
- H. C. Nash and C. S. Smith, J. Phys. Chem. Solids 9, 113 (1959).
- J. K. Percus and G. J. Yevick, Phys. Rev. 110, 1 (1958).
- J. C. Phillips and L. Kleinman, Phys. Rev. 116, 287 (1959).
- L. J. Sham and J. M. Ziman, "The Electron-Phonon Interaction" in Solid State Physics 15, edited by F. Seitz and D. Turnbull (Academic Press, New York, 1963).
- K. S. Singwi, M. P. Tosi, R. H. Land, and A. Sjolander, Phys. Rev. 176, 589 (1968).
- K. S. Singwi, A. Sjolander, M. P. Tosi, and R. H. Land, Phys. Rev. B1, 1044 (1970).
- J. C. Slater, Phys. Rev. 98, 1039 (1955).
- J. C. Slater, Phys. Rev. 81, 385 (1951).
- H. G. Smith, G. Dolling, R. M. Nicklow, P. R. Vitayarghavar, and M. K. Wilkinson, Inelastic Scattering of Neutrons in Solids and Liquids Vol. 1 (Vienna, IAEA) p. 149 (1968).
- F. Sun, R. Day, P. H. Cutler, and W. F. King, III, J. Phys. F: Metal Phys. 6, L1 (1976).
- F. Sun, private communications (1978).
- F. Toigo and T. O. Woodruff, Phys. Rev. B4, 371 (1971).
- M. P. Tosi, "Cohesion of Ionic Solids in the Born Model," in Solid State Physics 16, edited by F. Seitz and D. Turnbull (Academic Press, New York, 1964).
- A. D. B. Woods, N. B. Brockhouse, R. H. March, and A. T. Stewart, Phys. Rev. 128, 1112 (1962).
- W. W. Wood, "Monte Carlo Studies of Simple Liquid Models," in Physics of Simple Liquids, edited by H. N. V. Temperley, J. S. Rowlinson, and G. S. Rushbrooke (North-Holland Publishing Co., Amsterdam, 1968).
- W. W. Wood and F. R. Parker, J. Chem. Phys. 27, 720 (1957).
- J. M. Ziman, Phil. Mag. 6, 1013 (1961).
- J. M. Ziman, Principles of the Theory of Solids (Cambridge University Press, 1972).

DISTRIBUTION

Commander (NSEA 09G32)
Naval Sea Systems Command
Department of the Navy
Washington, D. C. 20362

Copies 1 and 2

Commander (NSEA 0342)
Naval Sea Systems Command
Department of the Navy
Washington, D. C. 20362

Copies 3 and 4

Defense Documentation Center
5010 Duke Street
Cameron Station
Alexandria, VA 22314

Copies 5 through 16